Global Assessment of Socio-Economic Drought Events at Sub-National Scale: A Comparative Analysis of Combined Versus Single Drought Indicators

Sneha Kulkarni[1], Yohei Sawada[1], Yared Bayissa[2], Brian Wardlow[3]

1 Department of Civil Engineering, School of Engineering, The University of Tokyo, Tokyo 113-8656, Japan

2 Department of Ecology and Conservation Biology, Texas A&M University, College Station, TX 77843, USA

3 School of Natural Resources, Center for Advanced Land Management Information Technologies, University of Nebraska–Lincoln, Lincoln, NE 68583, USA

Correspondence to: snehakulkarni@g.ecc.u-tokyo.ac.jp

Abstract. The accurate assessment of the propagation of drought hazards to socio-economic impacts poses a significant challenge and is still less explored. To address this, we analyzed a sub-national disaster dataset called the Geocoded Disaster (GDIS) and evaluated the skills of multiple drought indices to pinpoint global drought areas identified by GDIS. For the comparative analysis, a widely used Standardized Precipitation Index (SPI), Normalized Difference Vegetation Index (NDVI), Standardized Soil Moisture Index (SSMI), and Standardized Temperature Index (STI) were globally computed at the subnational level for the period 2001–2021. Out of 1641 drought events recorded in GDIS, NDVI identified 1541 (93.9%), SPI 1458 (88.8%), STI 1439 (87.7%), and SSMI 1376 (83.9%) events, respectively. NDVI showed better performance in highly vegetated areas due to its sensitivity to precipitation and soil moisture and its inverse relationship with temperature. Recognizing the limitations of single-input drought indices in capturing the complex propagation of droughts, we also introduced a novel Combined Drought Indicator (CDI), which integrates meteorological (rainfall and temperature), and agricultural (NDVI and Soil moisture) anomalies using a weighted approach to identify droughts and play a key role in minimizing inaccuracies in drought assessment. CDI successfully identified 1550 (94.5%) of the GDIS documented drought events, outperforming all individual indices. Based on CDI, the highest frequency of severe droughts (>7 events) was observed in sub-Saharan Africa and South Asia. It also captured persistent droughts in Argentina, Brazil, the Horn of Africa, western India, and north China; areas that are highly vulnerable to socio-economic droughts. Our findings highlight the importance of using CDI for improved identification of socio-economic drought events and for prioritizing regions at greater risk.

1 Introduction

Droughts are a complex phenomenon and have profound, long-lasting impacts on various sectors, including agriculture, water resources, industry, energy, and socio-economic conditions. For instance, in August 2021, a severe drought event affected 52% of crop yields in the Western United States, and in June 2019, Chennai, India, declared "day zero" due to almost no water remaining in all main reservoirs (Hossain et al., 2022). Climate projections indicate a future trend of increased frequency and severity in drought occurrences worldwide, amplifying their impacts on various sectors (Vicente-Serrano et al., 2022). These examples emphasize the urgent need for enhanced drought preparedness mechanisms and accurate drought impact assessment techniques in the coming years. When addressing drought assessment, one of the major challenges is understanding the exact propagation of drought hazard (meteorological/agricultural or hydrological) to its socio-economic repercussions.

Droughts do not have a specific, universally accepted definition. They are defined based on their association with different sectors and unique characteristics. Based on drought types and sectors, a number of drought assessment techniques and indices have been used worldwide to quantify and monitor drought conditions. To assess meteorological droughts, several indices such as the Standardized Precipitation Index (SPI) (Mckee et al., 1993), Standardized Precipitation Evaporation Index (SPEI) (Vicente-Serrano et al., 2010), and Temperature Condition Index (TCI)(Kogan, 1995) were extensively used. The World Meteorological Organization (WMO) recommends (Svoboda et al., 2012) SPI, which is widely used in many regions. For example, Bhunia et al. (2020), Blain et al. (2022), Kazemzadeh et al. (2022), Livada and Assimakopoulos (2007), Zhang et al. (2012) used SPI to asses droughts in Greece, the United Kingdom, Iran, India, and China, respectively. SPEI has been used in drought projection studies across the United Kingdom (Reyniers et al., 2023), the United States (Costanza et al., 2023), and the global (Vicente-Serrano et al., 2022) level, indicating an increase in severe drought events in these areas in the upcoming years. To assess agricultural droughts, the Standardized Soil Moisture Index (SSMI), Vegetation Condition Index (VCI), Normalized Difference Vegetation Index (NDVI), and Vegetation Health Index (VHI) have been widely recognized as effective indicators. Ding et al. (2022), Sandeep et al. (2021), and Tao et al. (2021) used the NDVI-based drought indices to perform detailed assessments of vegetation health and vigor in Australia, India, and China, respectively. Grillaki (2019) applied SSMI to reveal a significant rise in drought severity across Europe in recent years. Liu et al. (2022) investigated soil moisture dynamics in East Africa using a space-time perspective to identify the underlying causes of drought. Through a novel Eco-hydrological reanalysis, Sawada (2018) quantified the drought propagation from soil moisture to vegetation across the globe, highlighting that deeper soil layers exhibit delayed recovery from stressful conditions compared to shallow layers. To assess hydrological droughts and their impact on water resources and ecosystems, commonly used metrics include the Standardized Streamflow Index (SSI), Reservoir Storage Index (RSI), and Standardized Runoff Index (SRI). To understand surface water security, Mishra (2020) examined long-term trends in hydrological droughts across India using SRI. Forootan et al. (2019) conducted a global assessment of hydrological droughts, highlighting the strong regional impact of the North Atlantic Oscillation and Indian Ocean Dipole.

The studies mentioned above provided drought indicators that were based primarily on a single input variable or were sector-specific (either meteorological, agricultural, or hydrological). However, some works suggested that drought is a much more complex and multiphase phenomenon, resulting from various factors rather than just a single variable (Jiao et al., 2019a; Kulkarni and Gedam, 2018; Sepulcre-Canto et al., 2012). Hence, to understand droughts more accurately, the integration of multiple variables is needed, and it has a higher potential than single-variable-based traditional drought indices. This integrated approach can provide a more comprehensive understanding of droughts, considering the relationships between various contributing factors and the resulting impacts across different sectors. Recognizing the significance of combining multiple variables in drought monitoring, Svoboda et al. (2002) developed a drought monitoring system (US Drought Monitor) for the United States, which has been extensively used for regular practices in the United States. More recently, the near real-time Vegetation Drought Response Index (VegDRI) was developed and implemented in South Korea (Nam et al., 2018) and the USA (Brown et al., 2008), demonstrating more detailed and improved spatial drought patterns compared to multi-variable-based drought indicators. This VegDRI was developed by integrating eight climatic and biophysical datasets (SPI, Palmer drought severity index, performance of average seasonal greenness, start of seasonal anomalies, soil availability water capacity, irrigated agriculture, and ecological regions). In 2023, Guillory et al. (2023) developed the Australian Drought Monitor, integrating SPI, NDVI, soil moisture, and evapotranspiration, which has become a valuable tool in Queensland's official drought declaration process. Bayissa et al. (2019b), Huang et al. (2019), Kulkarni et al. (2020a), and Sepulcre-Canto et al. (2012) have developed and tested Combine Drought Indicators (CDI), demonstrating higher accuracy over Ethiopia, India, China, and Europe, respectively.

Droughts have significant socio-economic impacts, including crop losses, food insecurity, income reduction, water shortages, and displacement. The severity of these effects varies by region, depending on development level, infrastructure, and adaptive capacity. In high-income areas, systems like irrigation and insurance help reduce impacts, while in low-income regions, even moderate droughts can trigger crises (Brooks et al., 2005; Pak-Uthai and Faysse, 2018). Recent studies (Panwar and Sen, 2020; Udmale et al., 2014) highlight the importance of incorporating socio-economic vulnerability into drought assessments. However, the direct link between drought hazards and their socio-economic repercussions remains underexplored, partly due to the limited availability of reliable global impact data. Earlier efforts, such as the U.S. Drought Impact Reporter (National Drought Mitigation Centre, 2025), the European Drought Impact Report Inventory (European Drought Centre, 2025), and the European Drought Observatory (European Environment Agency, 2025), provided region-specific insights but lacked global coverage. To address this, the Geocoded Disaster (GDIS) dataset, developed from EM-DAT, offers geocoded disaster locations and detailed sub-national data on affected populations, fatalities, and economic losses. By overcoming previous limitations, GDIS enables spatial analysis of drought impacts across diverse socio-economic contexts.

Commented [SK7]: Technical Correction 10: Reviewer 3

Commented [SK8]: Revision based on Reviewer 2: Commen

100   Recently, the Geocoded Disaster (GDIS) dataset has been developed based on EM-DAT, offering geocoded disaster locations at a subnational level (Rosvold and H. Buhaug, 2021). By addressing the limitations of EM-DAT, the GDIS dataset provides detailed information on socio-economically affected areas and administrative units in GIS polygon format. In this paper, we used this newly developed GDIS dataset and show that it enables us to explore the less-understood link between drought hazards and their socio-economic repercussions more accurately and comprehensively.

105

Despite many works on single-variable and multi-variable drought indicators, very few have investigated how useful these indices are in globally exploring the links between drought hazards and their socio-economic repercussions. In this study, we globally applied four commonly used drought indicators, SPI, STI, NDVI, and SSMI, and compared these four traditional indices with GDIS to evaluate how well they represent the socioeconomic impacts of droughts. Then, inspired by the successful

110   regional examples of CDI, we also developed a new CDI on a global scale using two meteorological (rainfall and temperature) and two agricultural (soil moisture and NDVI) variables. To the best of our knowledge, very few studies (Hao et al., 2014a; Sánchez et al., 2018; Wang and Sun, 2023) have considered a global scale for their combined drought indicators, and none have compared and demonstrated the superior capability of such indicators over single-parameter-based traditional indices in global drought assessment. In addition, no studies have assessed the skill of drought indicators in identifying sub-national

115   socio-economic impacts globally, although the sub-national disaster dataset (i.e., GDIS) recently made it possible. In the present paper, we addressed the following key points.

1. Understanding the link between global drought hazards and their socio-economic impacts at the subnational scale using GDIS data.
2. Developing a new global combined drought indicator to enhance the precision and reliability of drought assessment (agro-climatological as well as socio-economic) and assessing its performance in detecting GDIS drought events.
3. Checking the performance of the commonly used traditional drought indicators (SPI, STI, NDVI, and SSMI) in identifying sub-national socio-economic impacts of droughts (i.e., their association with GDIS).

To achieve the stated objectives, our study was structured into three main components. Initially, we conducted an analysis of

125   global GDIS data to identify and select drought events at the subnational level. Later, a new global CDI was developed, and its performance in identifying GDIS events was assessed. Following this, we evaluated the effectiveness of four single-variable-based traditional indicators (SPI, SSMI, STI, and NDVI) in detecting the GDIS events compared to CDI. As a result, our research produced a comprehensive global framework for assessing drought impact, integrating agroclimatology hazard data with socio-economic impacts. This framework offers potential benefits for drought-prone regions worldwide, facilitating

130   improved drought management strategies and informed policy and decision-making processes.

2 Data

We used global observation and simulation data of rainfall, temperature, soil moisture, and NDVI to provide various drought indicators. These data sets were sourced from a combination of satellites and models and cover the time span from 2001 to 2021 on a monthly temporal scale. All the datasets had varying spatial resolutions. To address this disparity, we applied an Inverse Distance Weighted (IDW) method and rescaled all the datasets to a consistent resolution of 0.10° x 0.10°. All datasets were selected based on factors such as long-term data availability, accessibility, reliability, high spatial resolution, and overall data accessibility. To explore the linkage between drought indicators and socio-economic impacts, we used subnational disaster data. The subsequent paragraphs provide a detailed description of each dataset used in the study, and Table 1 outlines the respective sources of acquisition.

2.1 Rainfall

The monthly rainfall data were obtained from the Climate Hazards Group Infrared Precipitation with Station data (CHIRPS), developed by the U.S. Geological Survey (CHIRPS: Rainfall Estimates from Rain Gauge and Satellite Observations | Climate Hazards Center - U.C. Santa Barbara, 2023). We chose CHIRPS due to its high accuracy with station data, fine spatial resolution ($0.05° \times 0.05°$), and extensive temporal coverage from 1981 to the present.

2.2 Temperature

To understand the contribution of temperature to drought, the ERA5 Land temperature dataset (European Centre for Medium-Range Weather Forecasts, 2023) was used in this study. The average monthly gridded dataset was downloaded from the Copernicus Climate Data Store for the study period 2001 to 2021. The original spatial resolution was 0.1 x 0.1 degrees.

2.3 Soil Moisture

We used the ERA5 Land soil moisture dataset (European Centre for Medium-Range Weather Forecasts, 2023) acquired from the Copernicus Climate Data Store for the study period from 2001 to 2021. The monthly data products, with a spatial resolution of 0.1 x 0.1 degrees, were used for the study. The soil moisture datasets were available for different soil depth levels: first (0–7 cm), second (7–28 cm), third (28–100 cm), and fourth (100–289 cm). For our analysis, we used the first three layers (0–100 cm) to represent root-zone soil moisture, which is widely recognized in the literature (Bolten et al., 2010; Sawada, 2018; Sehgal et al., 2017) as critical for agricultural drought monitoring. To obtain a single representative value for soil moisture in the top 1 m, we employed a weighted averaging method using the respective thicknesses of the first three layers. The resulting weighted root-zone soil moisture layer was then standardized (e.g., using z-scores) and integrated into the CDI framework along with other drought-relevant indicators.

Commented [SK9]: Revision based on Reviewer 2: Commen

2.4 NDVI

NDVI serves as a significant indicator of vegetation stress levels. We used monthly NDVI data products from the Moderate Resolution Imaging Spectroradiometer (MODIS) spanning from 2001 to 2021. These data were obtained at a spatial resolution of 1 km, which we resampled to 0.1 x 0.1 degrees to align with other data sources for a comprehensive assessment. The MODIS NDVI dataset was used due to its global coverage and high temporal resolution, making it essential for monitoring vegetation health, facilitating timely detection, and assessing drought conditions worldwide.

2.5 GDIS/EM-DAT

Commented [SK10]: Technical Correction 15: Reviewer 3

The Global Disaster Identifier System (GDIS) dataset is a geocoded dataset distributed by SEDAC (NASA) that links disaster events to specific administrative boundaries (Rosvold and H. Buhaug, 2021). It builds upon the EM-DAT database by adding spatial GIS information, providing polygons for subnational regions affected by specific disaster events. Each event is tagged with the type of hazard (e.g., drought, flood, cyclone), the time period, and the affected regions at the sub-national level. In this study, only drought events were extracted from GDIS for the years 2001 to 2021. The GDIS dataset is based on the EM-DAT dataset. EM-DAT records a natural disaster when it meets any of the following conditions: 10 or more fatalities, impacts 100 or more individuals, or prompts a declaration of a state of emergency along with a request for international aid.

The use of GDIS, instead of relying solely on EM-DAT, adds spatial specificity and improves the ability to evaluate drought impacts in different regions, especially in developing countries where vulnerability is high. However, it's worth noting that GDIS coverage is not globally uniform and may be affected by underreporting in certain regions.

Commented [SK11]: Technical Correction 8: Reviewer 3

To identify any drought events from EM-DAT datasets, their event identifier (disaster number) information was extracted. In EM-DAT, disaster events are uniquely distinguished by the combination of an eight-digit disaster code and a three-digit country code, whereas GDIS employs only the eight-digit disaster code. Considering this common ground, GDIS drought events were shortlisted. In our study period, from 2001 to 2021, a total of 2142 GDIS-based drought events were identified. Since GDIS lacks drought start and end information, the exact yearly start and end information was acquired from EM-DAT. In some cases (143 events out of 2142 ~6.7%), due to the unavailability of monthly details in EM-DAT, we assumed January as the starting month and December as the end month of the respective event, and further analysis was carried out.

Commented [SK12]: Revision based on Reviewer 2: Comm

 Table 1. Details of the datasets used for this study.

Data	Description and source
Rainfall	CHIRPS data (original spatial resolution = 0.05° x 0.05°, further resampled to 0.1°*0.1°) (https://www.chc.ucsb.edu/data/chirps)
Temperature	ERA5-LAND data (spatial resolution = 0.1° x 0.1°) (https://cds.climate.copernicus.eu/cdsapp#!/dataset/reanalysis-era5-land-monthly-means)
Soil Moisture	ERA5-LAND (spatial resolution = 0.1° x 0.1°) (https://cds.climate.copernicus.eu/cdsapp#!/dataset/reanalysis-era5-land-monthly-means)
NDVI	MODIS (original spatial resolution = 1 km x 1 km, further resampled to 0.1° x 0.1°) (https://modis.gsfc.nasa.gov/data/dataprod/mod13.php)
GDIS	SEDAC NASA, (Original dataset- EMDAT), (spatial resolution – subnational level, temporal resolution – event-wise) (https://sedac.ciesin.columbia.edu/data/set/pend-gdis-1960-2018/data)

3. Method

3.1 Conventional single-variable-based drought indices

To understand the performance of drought indices in identifying GDIS drought events, we first employed four commonly used
individual variable-based traditional drought indices. These included the Rainfall-based SPI (computed using 'SPEI' and 'raster'
packages from R statistical software), Temperature-based STI, Soil Moisture-SSMI, and Vegetation Stress-related NDVI.
Drought assessments were conducted for all these indices on a monthly scale for the period from 2001 to 2021. Here, we
incorporated the standardization method (Z-score statistics) during index computation of SSMI, STI, and NDVI to facilitate
comparative analysis and noted similarities and differences between the results in identifying GDIS events. Z-score values
were computed using the following method,

$$Z\ Score = \frac{X - \mu}{\sigma} \tag{1}$$

where,

X = A specific value of a parameter within the set

μ = long-term mean

σ = long-term standard deviation

210 Further, the results for all four indices were classified and categorized, as shown in Table 2. The drought categories applied in this study follow the widely used SPI classification, originally developed by Mckee et al. (1993). Values ranging from zero to -2 or less (negative anomalies) indicate drought conditions, representing mildly dry to extremely dry situations. Conversely, values ranging from zero to 2 or greater (positive anomalies) depict mildly wet to extremely wet conditions, respectively. In this study, a 1-month accumulation period was used for SPI, STI, and SSMI to capture short-term drought dynamics. This

215 timescale is sensitive to rapid changes in agro-climatic conditions and supports early-stage drought detection. It also aligns with the monthly resolution of GDIS data, enabling accurate event-level analysis. The choice enhances consistency between drought indicators and the event database.

Commented [SK13]: Revision based on Reviewer 1: Comm 3

Commented [SK14]: Revision based on Reviewer 3: Comm 4

Table 2. Drought categories and specific class values used to evaluate the drought indices.

No	Index values	Drought category	Color Code	No	Index values	Drought category	Color Code
1	2 or more	Extremely Wet		5	0 to −0.99	Mildly Dry	
2	1.5 to 1.99	Severely Wet		6	−1.0 to −1.49	Moderately Dry	
3	1.0 to 1.49	Moderately Wet		7	−1.50 to −1.99	Severely Dry	
4	0 to 0.99	Mildly Wet		8	−2 or less	Extremely Dry	

220

3.2 Combined Drought Indicator

Commented [SK15]: Technical correction 1: Reviewer 1: T word 'combine' has been corrected to 'combined'

Various studies suggested that drought results from variations in multiple agro-climatological settings rather than just a single variable. The socio-economic repercussions of drought could occur due to combinations of multiple factors rather than a single

225 one. Hence, in this study, we developed a new combined drought indicator to assess droughts by considering multiple agricultural and climatological variables. We then checked and compared its association with GDIS events in the method described in Section 3.3. The CDI was developed using two agricultural variables (Soil Moisture, NDVI) and two climatological variables (Rainfall, Temperature). The CDI was generated as the weighted average of four independent drought indices shown in Section 3.1. The Principal Component Analysis (PCA) technique was used to assign weights to all four input

230 indices. PCA has been widely used in atmospheric and hydrological studies to describe dominant patterns in multivariate data. The PCA method was selected for constructing the CDI due to its ability to extract dominant patterns of variability across multiple input indices without requiring a dependent variable. This makes it particularly suitable for integrative assessments across diverse drought types and geographic regions. Compared to other commonly used weighting methods, such as the Analytic Hierarchy Process (AHP), which relies on expert judgment (Saaty, 1980), or entropy weighting, which uses the

235 diversity of information in data (Mahato et al., 2023), PCA offers an objective, data-driven approach that reduces subjectivity. While regression-based methods have also been explored to link drought indicators with socio-economic impacts (Hao et al., 2014b), they typically require clearly defined response variables and may introduce model-based biases. In contrast, PCA

generates uncorrelated components and assigns weights based on explained variance, enhancing reproducibility and generalizability in global-scale assessments.

240

In this study, the PCA technique was used to assign monthly weights to the four input indices: SPI, STI, SSMI, and NDVI. PCA is commonly used in environmental and climate studies to extract dominant patterns in multivariate datasets without requiring a dependent variable. In this study, PCA was conducted separately for each calendar month using time series data from 2001 to 2021, resulting in 21 observations per variable. Although the number of observations is relatively modest, it
245 satisfies the commonly accepted subject-to-variable ratio of at least 5:1 for PCA (Jolliffe, 2002; Gorsuch, 1983), especially when the number of variables is low, and the objective is dimensionality reduction. Through PCA, new orthogonal (independent of each other) variables, i.e., P.C.s, were constructed using linear combinations of the original indices without significant loss of information. The first principal component (PC1), which captures the highest variability in the input data, was selected for further analysis. In PCA, principal components are calculated to maximize the variance explained, and the
250 total of the squared loadings (eigenvectors) equals one. These squared loadings indicate each variable's contribution and were used to derive monthly weights for each input index. Using this approach, we generated 48 spatially weighted maps (12 months × 4 variables). The percentage weights obtained from PCA were then used to compute the CDI as follows:

Weighted CDI(i,j)= WtSPI(i) × [SPI](i,j) + WtSTI(i) × [STI] (i,j) + WtSSMI(i) × [SSMI](i,j) + WtNDVI(i) × [NDVI](i,j)

(2)

Where WtSPI, WtSTI, WtSSMI, and WtNDVI represent the weights for the i-th month (January to December) for their
255 respective parameters. These weights were multiplied by the individual index values for the j-th year and i-th month, and then all the values were added to obtain the CDI results for the i-th month and j-th year. Finally, all the CDI results were normalized for comparative analysis. This normalization process was carried out using the following formula:

$$CDI(i,j) = \frac{weighted\ CDI(i,j)}{\delta(i)}$$ (3)

Where, CDI(i,j) represents the combined drought anomaly for the i-th month and j-th year, while $\delta(i)$ denotes the standard deviation for the i-th month across all years (2001 to 2021). The CDI results were shown using the same color scheme and
260 drought categories, as depicted in Table 2. Figure 1 illustrates the schematic flowchart outlining the process for computing PCA-based CDI.

In the later stage, the same process as that for individual indices (SPI, STI, SSMI, NDVI) outlined in section 3.1 was followed to assess the association between CDI results and GDIS drought events. Similarities and differences observed by CDI in
265 identifying GDIS events compared to SPI, STI, SSMI, and NDVI across various temporal scales and with different criteria were examined. Detailed explanations of these results are provided in the following section.

Commented [SK16]: Revision based on Reviewer 1: Comm 5

Commented [SK17]: Revision based on Reviewer 1: Comm 6

3.3 Evaluation of the drought indices by GDIS

We assessed the number of events among the shortlisted GDIS drought events (see Section 2.5) that were detectable by each drought index. This analysis suggests how well each index detects socio-economic stress during droughts. This analysis was performed using ArcMap 10.8. The GDIS polygons were overlaid onto the gridded drought index (SPI, STI, SSMI, NDVI, and CDI) layers separately to extract spatial and temporal raster-based information for each drought event. A total of 2,142 events recorded between 2001 and 2021 were analyzed. Event-specific details such as location and start and end dates were obtained from the GDIS and EM-DAT databases. For each drought event, index values were extracted from the respective raster datasets based on the spatial extent (polygon) and duration of the event. For example, if a GDIS event occurred in Bihar, India, from March to December 2012, the relevant monthly raster values for SPI, STI, SSMI, NDVI, and CDI within the Bihar polygon during that period were extracted.

To align the gridded drought indices with the spatial scale of the GDIS events, we computed the monthly spatial average of each drought index over all grid cells within the corresponding event polygon. This process produced a single time series per index for each event. The resulting geodatabase tables were then analyzed to assess whether the index values were consistent with the GDIS records. Following previous literature (McKee et al., 1993; Bayissa et al., 2019a; Kulkarni et al., 2020b), a threshold of ≤ -1 was used to define moderate to extreme drought conditions (Table 2). A drought index was considered consistent with a GDIS event if the average value of the index within the event polygon was ≤ -1 in any month during the event's duration. For instance, if the average STI value within the Bihar polygon fell below -1 in any month between March and December 2012, STI would be considered consistent with that GDIS event. To evaluate sensitivity, a secondary analysis was also conducted using a threshold of < 0. In this case, if any monthly average value of an index was below zero during the event, it was also marked as consistent. This two-threshold approach allowed for both conservative and more inclusive assessments of drought index performance against GDIS events. For clarity, a stepwise procedure of thresholding and spatial averaging is presented in Appendix A.

The occurrence of GDIS events (socio-economic repercussions) may not solely originate from conditions in a particular month but could also reflect agro-climatological stress conditions from the preceding one, two, or three months. Hence, we also analyzed the GDIS events and their association with all five indices by adjusting the duration of event occurrences. We conducted additional analysis by extending the data extraction timeframe for all five indices. For example, in Bihar, India, for the GDIS drought event from March to December 2012, we not only extracted index data for March to December 2012 but also for one month before the event (February), two months prior (January), and three months prior (December 2011) for SPI, STI, SSMI, NDVI, and CDI and checked if the index anomalies are consistent to GDIS or not in any of these durations.

Commented [SK18]: Revision based on Reviewer 1: Comm 7

Commented [SK19]: Revision based on Reviewer 1: Comm 8

Research suggests that the shorter-duration dry periods have significant importance for various socio-economic applications, such as water availability and energy sources in adjacent months (Christian et al., 2021, 2024; Mukherjee and Mishra, 2022). Hence, during the shortlisting process of the 2142 GDIS drought events from the entire natural disaster dataset, the initial criteria were to consider all the events, including short droughts (droughts lasting more than one month or up to two months). Consequently, in the later stage of this research, to comprehend the importance and differences in the selection of timescales, the initial criteria were slightly adjusted. Instead of considering all events, only events lasting more than or equal to two months were examined. This criterion was established to mitigate the impact of short-term changes and biases in results caused by short droughts or smaller dry periods. After the implementation of these criteria, we got 1641 GDIS drought events.

To summarize, the comparative analysis of GDIS with all the conventional indices (SPI, STI, SSMI, and NDVI) and CDI was carried out based on 1) two types of drought events, those lasting greater than or equal to two months and all events, including those with shorter durations (i.e., less than two months). 2). During this process, four temporal data scales were considered: the actual event period, data from one month prior to the event, data from two months prior to the event, and data from three months prior to the event. 3) For all the indices, events were classified as drought if the values were below 0 (in the first case) and below -1 (in the second case); the remaining events were marked as non-drought events.
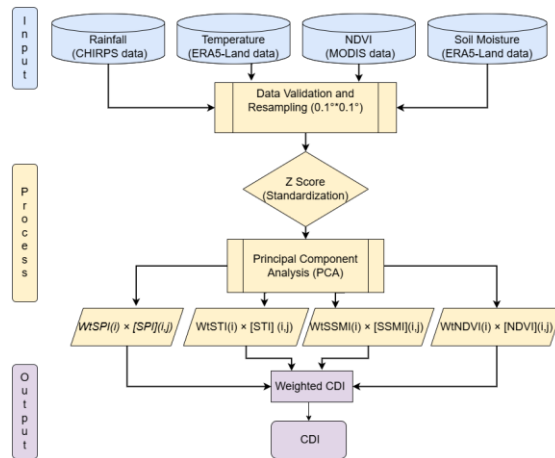
Figure 1. The general flow of the method followed to compute CDI-based droughts. Here, i represent the month from January to December, and j indicates the years from 2001 to 2021.

4. Results

4.1 Global Drought Frequency Analysis by GDIS Events

The GDIS dataset contains location data for 39,953 events globally, including various natural disasters such as extreme temperatures, floods, mass movements, storms, droughts, and earthquakes. Among these, 2,142 events were explicitly identified and classified as drought events. Figure 2a illustrates the global spatial distribution of drought frequencies of all 2,142 GDIS drought events. The highest number of these drought events was recorded in Africa (779; 36.37%) and Asia (710; 33.15%), followed by the Americas (477; 22.26%), Europe (106; 4.95%), and Oceania (70; 3.27%). Analyzing drought frequencies at a finer scale, Djibouti in Africa reported the highest frequency of GDIS drought events (8 occurrences), followed by Ethiopia and Kenya (7 occurrences each) and Somalia (6 occurrences) (Fig. 2b). In the Americas, Bolivia recorded the highest number of GDIS drought events in South America, while Honduras had the highest frequency in Central America (7 occurrences). In North America, Kansas County in the USA documented the highest number of GDIS drought events (4 occurrences), followed by California, Arizona, and Illinois with three occurrences each (Fig. 2c). In Asia, the Nei Mongol administrative unit in China documented the highest frequency of GDIS drought events (7 occurrences). This is followed by several administrative units in Thailand, including Chaiyaphum, Loei, Nan, and Kalasin, which each recorded a high frequency of GDIS drought events (6 occurrences), indicating a significant vulnerability to drought in these regions. Additional regions in China (such as Yunnan, Shanxi, and Hebei), India (Maharashtra and Andhra Pradesh), and Cambodia (Pursat and Kampong Speu) documented moderate GDIS drought frequencies (3 to 5 occurrences) (Fig. 2d).

On the temporal scale, parts of Africa and South America experienced the highest extended drought events. The drought over Burundi, Africa, lasted continuously for two years from 2004-2006, whereas the drought in South America, over Honduras, lasted for around a year in 2009. Some of these events were very harshly socio-economically devastating. EM-DAT data showed that, in a major event in Africa, nearly 2 million people were affected, whereas in Thailand, around 3 million people faced the impacts of drought.

It is also noteworthy that areas with low population density, like Western Australia or Central and Western Russia, did not experience any GDIS events. In contrast, higher population areas were more prone to GDIS events, making population density a key factor in socio-economic stress. Additionally, it was observed that areas with smaller spatial scales are less likely to experience GDIS events compared to larger areas.

Commented [SK20]: Technical correction 2: Reviewer 1: legend has been added to Figure 3a

345
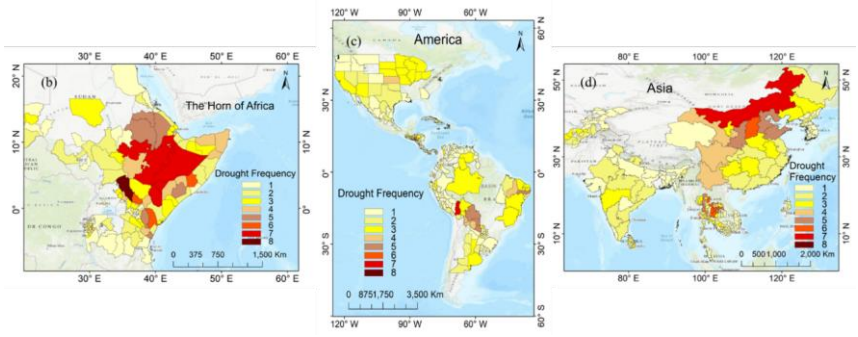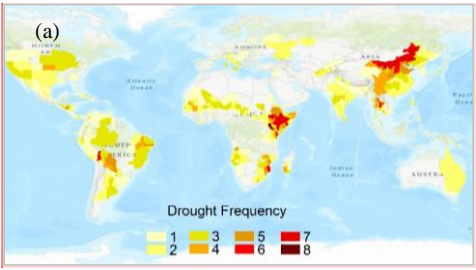
Figure 2. Spatial distribution of GDIS drought frequencies: (a) Global scale, (b) East Africa, (c) America, and (d) Asia. The drought frequencies range from one to eight, represented by shades from light yellow (low frequency) to dark brown (high frequency). Note: The color scheme used here is distinct from the CDI classification shown in Table 2 and represents event frequency, not drought intensity.

Commented [SK21]: Technical Correction 1: Reviewer 2: Figure caption modified

350 **4.2 Performance of CDI in detecting GDIS events.**

In the computation of the CDI, one of the initial steps involves assigning weights to all input variables using the PCA method. Figure 3 shows the pixel-based weights for each variable for the sample month of April. Similar weights were computed for all twelve months across four input variables (Appendix B: Rainfall- Fig. B1, Temperature-Fig. B2, NDVI-Fig. B3, and Soil Moisture- Fig. B4). In April, the highest weights were assigned to soil moisture, indicating its greater contribution to the

355 development of CDI compared to NDVI, LST, and rainfall. Lower weights were assigned to LST, suggesting a weaker correlation with other variables and a lesser role in CDI formation for April. Significant variations in these weights have been observed across different global regions, reflecting seasonal dynamics. In the tropical areas of Southeast Asia and parts of Africa, rainfall and soil moisture exhibit higher weights during the monsoon seasons from June to September, while NDVI becomes more prominent in the subsequent months. Whereas, in parts of North America, NDVI shows higher weights in

360 September and October, followed by soil moisture and rainfall (Appendix B).
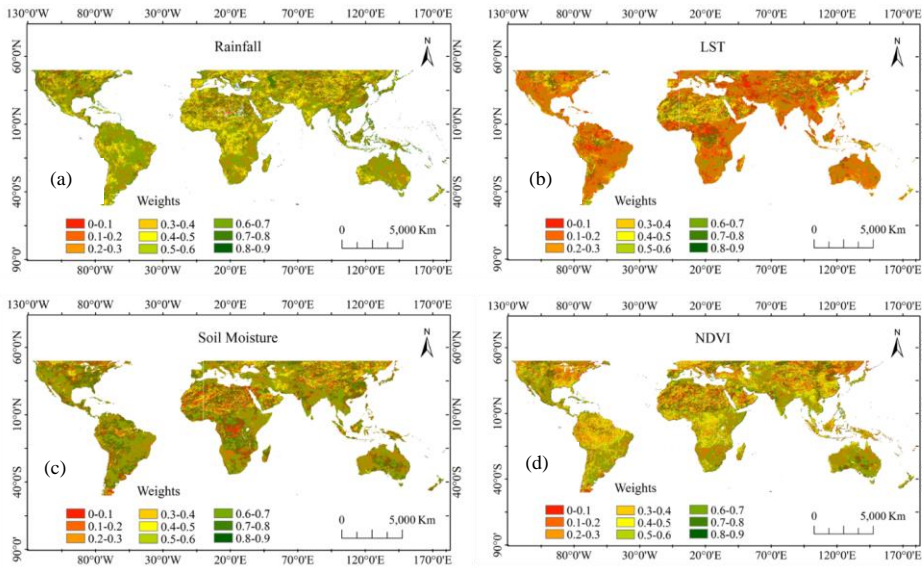
Figure 3. Example of pixel-based weights for the four input variables of CDI: rainfall (a), LST (b), soil moisture (c), and NDVI (d), calculated using the PCA method for a sample month (April). The weights range from 0 to 1, with colors varying from dark red (lower weights) to dark green (higher weights).

The CDI maps helped to identify different categories of droughts between 2001 and 2021 over various regions of the globe (Appendix C). Severe to extreme drought conditions were observed over South African countries such as Malawi and Zambia, as well as the Horn of Africa, including Ethiopia, Kenya, and Somalia, during 2015-16. In the United States, the years 2007-08 and 2012 were marked as severe to extreme drought years, affecting the southeastern states and the Midwest, respectively. During November 2009, the CDI noted one of the most destructive drought periods in northern and western China. The year 2015 was marked by the CDI as a severe drought year in India, affecting 52% to 67% of the region and causing massive agrarian stress. Additionally, the CDI data indicated that during early 2019, areas of Australia, particularly Queensland and New South Wales, experienced some of the most severe drought conditions recorded in recent years. Further, overlapping the GDIS polygons on these CDI results helped to understand the association between CDI and GDIS drought events.

Figure 4 demonstrates the performance of CDI in detecting GDIS events. Figure 4a shows CDI for North and Central America in June 2015 overlaid with black polygons representing GDIS data for the same period. Similarly, Figures 4b and 4c showcase the CDI maps for Africa in June 2009 and South America in August 2009, respectively, aligning with periods of reported GDIS events with their corresponding polygons. In these examples, it is clearly seen that GDIS polygons are exactly aligned with severe to extreme drought areas, as noticed through the base maps of CDI. Likewise, out of a total of 2142 GDIS global

drought events with actual event period (AEP), CDI can detect 1885 (88%) drought events when the drought criteria were set to -1 or less and 2117 (98.83%) when the criteria were set to 0 or less. After adjusting the criteria to consider drought events lasting two months or longer, the total event count was reduced to 1641 GDIS events. Under this criterion, CDI identified 1550 (94.45%) GDIS events when the drought threshold was set to -1 and 1635 (99.63%) when the threshold was set to 0. Adjusting the criteria and thresholds more rigorously (one month prior to the end of GDIS events, two months prior to the end of GDIS events, and three months prior to the end of GDIS events) resulted in a stronger association between GDIS and CDI, with percentages ranging from 91% to 100% (Table 3). In the first criterion, when considering one month prior to the AEP and using a threshold of -1, CDI detected 1,954 events, accounting for 91.22% of the total. When the threshold was changed to 0, 2,130 events (99.44%) were identified by CDI in alignment with GDIS. When short-duration drought events were excluded under the same criterion, CDI detected 1,573 events (95.86%) at the -1 threshold and 1,637 events (99.76%) at the 0 threshold. Under the second criterion, when two months prior to AEP, CDI detected 2,010 events (93.84%) using a threshold of -1, and 2,137 events (99.77%) when the threshold was adjusted to 0. Excluding short drought events in this scenario, CDI identified 1,587 events (96.71%) at the -1 threshold and 1,637 events (99.76%) at the 0 threshold. In the final criterion, considering three months prior to AEP, CDI detected 2,042 events (95.33%) at the -1 threshold and 100% of events at the zero threshold. After excluding short drought cases, 1,589 events (96.83%) were captured at the -1 threshold, and again, all events (100%) were identified at the 0 threshold. Among the shifting windows, the three-month prior criterion with a threshold of 0 demonstrated the highest detection rate, capturing 100% of GDIS events. However, this also suggests a higher likelihood of false alarms, as early indicators may not always align with actual drought impacts.

These results highlight that GDIS events, which appear to occur in specific months, may actually be the outcome of agro-climatic variability occurring one, two, or even three months prior to the reported event, rather than being confined to that specific month alone.

Commented [SK22]: Technical Correction 22: Reviewer 3

Commented [SK23]: Technical Correction 25: Reviewer 3
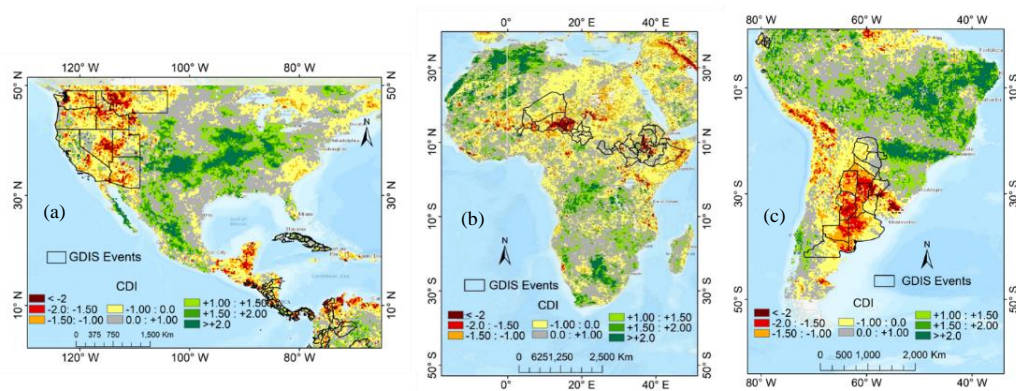
Figure 4. Assessment of Drought Using CDI with Overlay of GDIS Events over America (June 2015) (a), Africa (June 2009) (b), and South America (August 2009) (c). The black polygons represent GIS polygons from GDIS, indicating drought-affected administrative units based on GDIS data. The base maps display CDI results for the respective GDIS drought months, ranging from dark brown (indicating extreme dry conditions) to dark green (indicating extreme wet conditions). The alignment of GDIS polygons with droughts detected by CDI demonstrates the CDI's capability to accurately identify GDIS droughts during the respective periods.

Table 3. Performance of CDI in detecting GDIS events using multiple criteria.

CDI vs GDIS	Total Event	Drought Criteria	Actual Event Period (AEP)		One Month Prior + AEP		Two Month's Prior + AEP		Three Month's Prior + AEP	
			-1	0	-1	0	-1	0	-1	0
Including	2142	Observed	1885	2117	1954	2130	2010	2137	2042	2142
Short		%	88.00	98.83	91.22	99.44	93.84	99.77	95.33	100
Drought		Not Observed	257	25	188	12	132	5	100	0
		%	12	1.17	8.78	0.56	6.16	0.23	4.67	0
No Short	1641	Observed	1550	1635	1573	1637	1587	1637	1589	1641
Drought		%	94.45	99.63	95.86	99.76	96.71	99.76	96.83	100
(event >=2		Not Observed	91	6	68	4	54	4	52	0
months)		%	5.55	0.37	4.14	0.24	3.29	0.24	3.17	0

405

410

415

Figure 5 illustrates the performance of CDI in detecting GDIS drought events across different regions (Appendix D represents the performance of traditional indices). In this analysis, the drought identification criteria were set as all GDIS events, including short-duration cases, with a drought threshold set at -1 or less. Out of a total of 2,142 GDIS events, the highest number was observed in Africa, with 779 events, of which CDI successfully detected 678 (87.03%). Following Africa, South and Southeast Asia experienced 613 (78.69%) GDIS drought events, with CDI accurately identifying 526 (67.52%) of these. In South and Central America, there were 434 GDIS drought events, and CDI identified 387 (89.17%) of them. East Asia and the Pacific saw 144 GDIS events, with CDI detecting 138 (95.83%). Europe and Central Asia, as well as Northern America, had the fewest GDIS events. CDI detected 111 events in Europe and Central Asia and all 53 events in Northern America. These findings indicate that CDI exhibits high accuracy in regions with larger subnational scales compared to areas with smaller scales. The 100% detection rate of GDIS droughts in Northern America by CDI may be attributed to the extensive area extent of the region. In line with our results, a previous study by Kageyama and Sawada (2022) also showed that developed countries are easier to detect. These countries did not suffer from droughts without strong climatological hazard signals, which enhances the capability of our climatology-based hazard index. The vast subnational scale of Northern America includes a greater number of CDI image pixels, which likely enhances the correlation with GDIS events.

Despite the higher association of CDI in detecting GDIS events, there were a few instances (e.g., Burundi, and parts of Thailand) where CDI failed to capture GDIS events. The smaller spatial extents (subnational scales in Southeast Asia or parts of Africa) could be one reason for this discrepancy. Additionally, these regions might be experiencing other types of stress beyond agro-climatological factors (as indicated by CDI) that contribute to the GDIS events. It was also found that CDI identified stress conditions in some locations that were not reflected in GDIS. For instance, CDI detected severe drought events in South Argentina during 2014–15, Namibia in 2013, and parts of Europe in 2018, which were not reflected in GDIS event records. These instances highlight that; not all agro-climatic droughts lead to recorded socio-economic impacts, especially in regions with strong adaptation and mitigation capacities. Practices such as advanced irrigation, drought-resistant crop varieties, or effective early warning systems may help manage the agricultural and societal impacts of climatic stress, thereby reducing the likelihood of such events being recorded in GDIS. It is also important to note that GDIS does not comprehensively capture all real-world drought events, particularly in regions with limited reporting mechanisms or institutional capacity. As a result, some drought events, especially in low-income or remote areas, may go undocumented despite having significant local impacts.

Commented [SK24]: Technical Correction 18: Reviewer 3

Commented [SK25]: Revision based on Reviewer 2: Comm 3
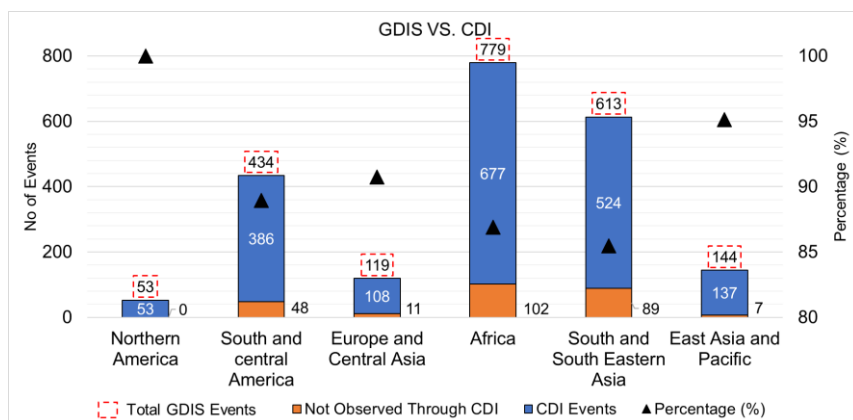
Figure 5. Performance of CDI in Detecting GDIS Events Across Different Geographic Regions. A total of 2142 drought events were identified from GDIS. CDI successfully detected events marked in blue, with counts indicated by red dotted boxes. Events missed by CDI are represented in orange. The black triangles indicate the percentage of GDIS events captured by CDI.

4.3 Comparative Assessment of CDI and individual parameter-based traditional indices

Figure 6 presents a comparative analysis of multiple drought indices, including CDI, in detecting GDIS events using various criteria. When considering the initial criteria (Fig. 6a), which covers the actual event period of GDIS and includes all events, including short-duration droughts, a total of 2142 events were identified in GDIS. Among these, CDI exhibited the highest detection rate with 1885 (88%) events, followed by NDVI with 1867 (87.16%) events, SSMI with 1770 (82.63%) events, SPI with 1740 (81.23%) events, and STI with 1650 (77.03%) events. Here, the criterion was set to consider all events, including short-term drought occurrences, with the drought threshold set to -1 or lower. The number of the GDIS drought events captured by each index can easily be increased by the lower threshold of drought identification (Fig. 6a, 6b, 6c, 6d, and subplot 2), although it inevitably increases the false alarms. This association remained consistent when the drought criteria were further refined to exclude events shorter than two months (Fig. 6a, 6b, 6c, 6d, and subplot 2). It's also notable that the agricultural indices (NDVI and SSMI) exhibit greater efficacy in identifying GDIS drought events compared to meteorological indices (SPI and STI). This suggests that they may offer a more accurate representation of socio-economic conditions. Through this analysis, we observed that NDVI performs better in regions with diverse vegetation cover and seasonal variability, such as the Indian subcontinent and South America (Appendix E). In contrast, SSMI detected more drought events than NDVI in semi-arid areas like Central Asia (e.g., Kyrgyzstan, Afghanistan), where NDVI is less informative due to sparse vegetation.

When considering an alternative criterion that includes drought data spanning two months prior to the onset of the GDIS event until its end date, with the exclusion of short-term drought occurrences, a total of 1641 GDIS events were observed. Out of these 1641 events, CDI demonstrated the highest efficacy by detecting 1587 (96.71%) events. Subsequently, NDVI identified 1574 (95.91%) GDIS events, while SSMI detected 1580 (96.28%) events. SPI observed 1550 (94.45%) events, and STI represented 1510 (92.02%) events, showcasing its lesser capability in detecting GDIS events. It is observed that, across most criteria (Fig. 6b, 6c, 6d), CDI demonstrated a superior capability in identifying GDIS events compared to other indices. It is also observed that, across most criteria, the CDI has a greater potential to detect GDIS droughts compared to traditional drought indices based on single input variables (Appendix F: Table F1, Table F2, Table F3, and Table F4).

However, there were three instances where CDI lagged other indices, primarily NDVI or SSMI, in detecting GDIS events. In the first scenario (Fig. 6b, criterion: one month prior to AEP and including short droughts), CDI detected 1954 (91.22%) GDIS events, while NDVI identified 1983 (92.58%) GDIS events. Similarly, in the second scenario (Fig. 6b, criterion: two months prior to AEP and including short droughts), NDVI maintained its superiority in detecting GDIS events, observing 2028 (94.68%) events compared to CDI's detection of 2010 (93.84%) events. In the third scenario (Fig. 6c, criterion: three months prior to AEP and no short droughts considered), although CDI detected 1589 (96.83%) GDIS events, SSMI outperformed by observing 1610 (98.11%) GDIS events. These discrepancies may be caused by CDI giving more weight to input parameters such as SPI and STI, influenced by regional variability, local environmental conditions, and land cover patterns during these event periods.

For comparative analysis of drought detection performance, recall serves as a crucial metric, as it quantifies the ability of each index to correctly identify actual drought events. High recall is especially important in early warning systems, where missing events can lead to unmitigated impacts. As illustrated in Appendix G, the CDI index consistently outperforms others across all time windows, particularly for events lasting ≥2 months, where it achieves recall values between 0.94 and 0.97, demonstrating robust and reliable drought detection capability. For a more comprehensive understanding of detection performance, additional metrics derived from a full confusion matrix, such as precision, specificity, and F1-score, could provide further insights and represent a promising direction for future work.

Commented [SK26]: Revision based on Reviewer 2: Comm 6
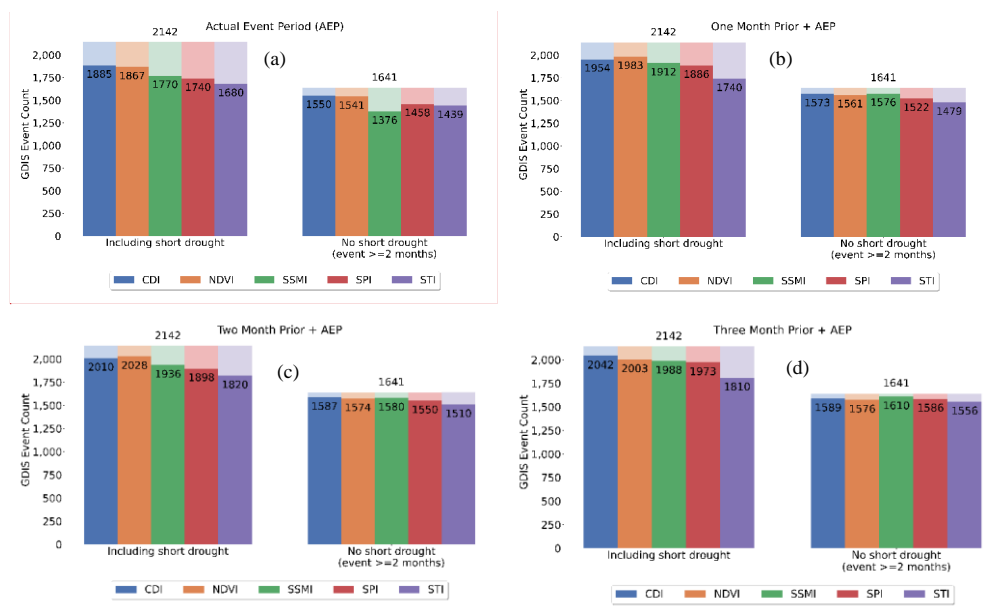
Figure 6. Comparative Assessment of CDI vs Traditional Drought Indices in Detecting GDIS Droughts (Drought Identification Threshold: -1 or less). The first subplots of a, b, c, and d illustrate the performance of indices in detecting droughts from a total of 2142 GDIS drought events (considering short drought events). The second subplot of a, b, c, and d shows the performance of indices in detecting GDIS drought events when short drought events are excluded, resulting in a total count of 1641. Actual Event Period (AEP) is the exact period when the GDIS event occurred, for which index data has been considered. One month, two months, and three months+ AEP are the respective previous months relative to GDIS events plus the actual event period from which index data was considered to understand the lag effect in GDIS event occurrences.

Commented [SK27]: Technical Correction 2: Reviewer 2: Replaced with the new image

One of the reasons for the superiority of CDI in detecting GDIS drought events is its flexibility.CDI can be tailored to suit local or regional contexts, taking into account the unique characteristics represented by specific traditional indices or combinations of multiple indices. Figure 7 provides examples of such cases, where one or more individual indices represented GDIS drought events, allowing CDI to also detect those GDIS events. Figure 7a shows one of the event cases over Busoni, Burundi, from Africa, where the GDIS event was observed from April 2014 to September 2014. In this case, the lines for NDVI, SPI or STI didn't cross the drought threshold (-1) during the particular period, hence couldn't detect the GDIS event. SSMI could detect this drought, and CDI has a relatively large weight on SSMI, so CDI could also detect it. The average rainfall is low with small variability over this region in this period, making SPI not detecting this event, whereas the common hot and semi-arid climate of this region would not have helped STI and NDVI to detect drought over Burundi. The decreased availability of groundwater or surface water in this area likely resulted in reduced soil moisture supply, contributing to SSMI

drought. In the second example (Fig. 7b), a GDIS drought event was observed over Gaya, Bihar, India, from May 2009 to
510   September 2009. This region is located along the banks of the Ganga River, which is likely to provide ample irrigation.
Consequently, SSMI and NDVI did not indicate a drought in this area. However, the insufficient rainfall over Gaya during this
period caused socio-economic stress, which was detected by both SPI and CDI.

Figure 7c shows the performance of various indices over Holguin, Cuba, where a GDIS event was reported from August 2004
to March 2005. In this case, STI and SPI did not detect the drought, whereas NDVI and SSMI indicated drought conditions,
515   leading to the CDI's detection of the drought as well. Despite non-drought conditions in precipitation and temperature,
agricultural stress factors such as poor vegetation health or subsurface water depletion could have contributed to this drought,
which was effectively captured by NDVI, SSMI, CDI, and GDIS. In the fourth example (Fig. 7d), a GDIS event was observed
over Nebraska, USA, from June 2012 to November 2012. All five indices (NDVI, SSMI, STI, SPI, and CDI) detected this
event, highlighting the extreme drought severity during this period in the USA.

520
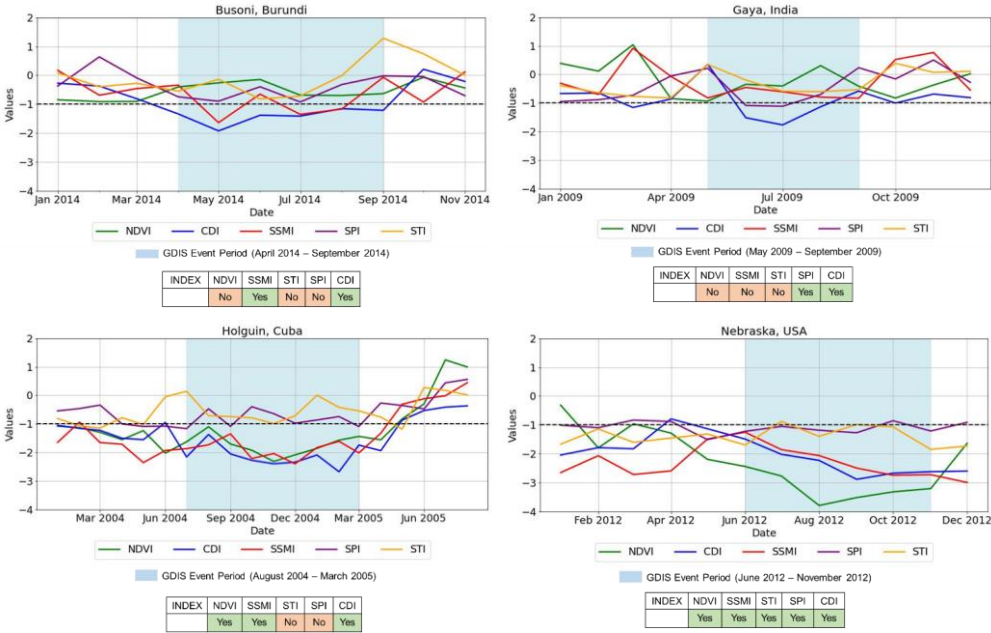
Figure 7. Performance of CDI, SPI, STI, SSMI, and NDVI in detecting GDIS events over Burundi, Gaya, Holguin, and Nebraska. The blue
boxes denote the duration of GDIS events, while colored line graphs represent the index values of NDVI (green), CDI (blue), SSMI (red),
SPI (purple), and STI (yellow). If the line of any index value crosses the drought threshold of -1 (dotted black line) during the specified
GDIS event period (blue box), that index is considered capable of identifying the GDIS drought event.

Figure 8 represents the zonal validation results for drought index performance across four climate zones (Arid, Tropical, Temperate, and Cold) based on Köppen's climate (Peel et al., 2007) classification (threshold criterion: -1). The figure highlights how different indices perform differently under varying climatic conditions, while the CDI demonstrates consistently high detection accuracy across all zones. In the Arid zone (a), CDI detected 95.4% of GDIS events (the highest among all indices), while SSMI and NDVI also performed well with 93.0% and 90.5%, respectively. This can be attributed to the high sensitivity of NDVI and SSMI to vegetation and soil moisture stress, which are obvious under arid conditions. However, in the Cold zone (d), individual index performance dropped noticeably, with SPI detecting only 66.0% of events, whereas CDI still maintained 80.3% detection. Similarly, in the Temperate zone (c), both CDI and SSMI showed strong association with GDIS at 87.2% and 89.2%, respectively, indicating that some indices may be better suited for certain climate types. In contrast, the Tropical zone (b) showed relatively lower detection percentages for all indices, with CDI still leading at 80.9%. SSMI performance in tropical and cold zones was lower, possibly due to dense vegetation cover and higher variability in surface moisture, which can limit the accuracy of soil moisture retrievals. These results emphasize that while individual indices can perform well in specific climate zones, their performance is not consistent across all zones. CDI, by integrating multiple indicators, offers more universally reliable detection, making it better suited for broader applications in drought monitoring across diverse climatic regions.
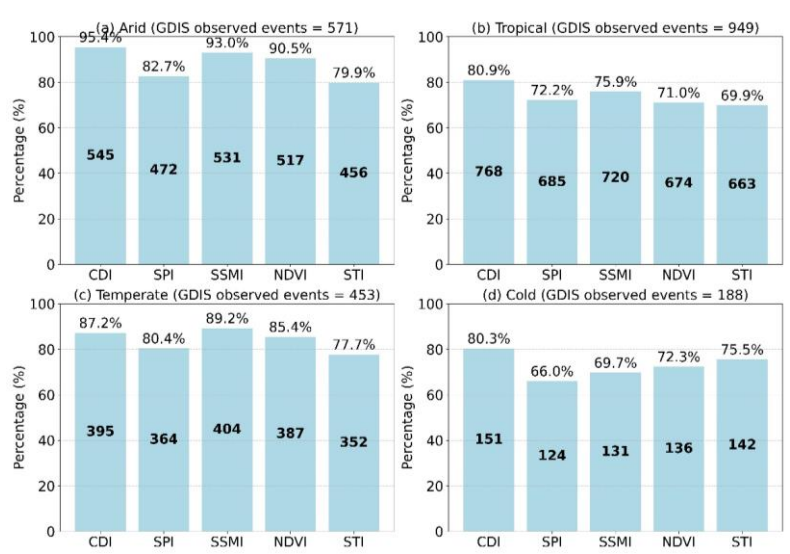
Figure 8. Zone-wise accuracy of drought indices (CDI, SPI, SSMI, NDVI, STI) in detecting GDIS events across four Köppen climate zones: Arid, Tropical, Temperate, and Cold. The bar heights represent the percentage of GDIS events accurately captured by each index (threshold = -1), and the numbers inside the bars indicate the absolute number of consistent detections. The total number of GDIS events considered per zone is: Arid – 571, Tropical – 949, Temperate – 453, Cold – 188 (Total = 2161).

545 Similarly, we performed a zonal validation of drought index performance across major land cover classes, Forest, Shrubland and Savanna, Agriculture and Cropland, Settlement, and Barren lands, based on MODIS land cover data. As shown in Appendix H, the results indicate that CDI consistently outperformed individual indices across all land cover types in detecting GDIS events. This reinforces the robustness of CDI in capturing multi-dimensional drought signals, even across heterogeneous land surface conditions.

550 To better understand the spatial behavior of the CDI, a correlation analysis was performed (Fig. 9) to examine how consistently each input index aligns with the composite signal across regions. In general, strong correlations were observed between CDI and SSMI, followed by NDVI, SPI, and STI among the four single input-based traditional indices. CDI was highly associated with SSMI over the Indian subcontinent, Australia, and South America. However, these correlations exhibited spatial and temporal variability. Monthly assessments revealed significant seasonal variations in the correlations between CDI and other

555 indices. During monsoon months (June, July, August, and September), CDI exhibited a higher correlation with SPI over the Indian subcontinent compared to non-monsoon months. Similarly, in arid regions of Africa, strong correlations between NDVI, SSMI, and CDI were observed during rainy months (June to September), which diminished during dry months. As a sample example, Figure 9 depicts the spatial correlation between CDI and other indices in the sample month of April. On average, NDVI exhibited a higher correlation with CDI, particularly in northern America, southern parts of Africa, and the Indian

560 subcontinent. Following NDVI, SSMI and SPI demonstrated stronger associations with CDI. However, in April, CDI exhibited a lower correlation with STI. Parts of South America, South Africa, Australia, and the Indian subcontinent even displayed a negative correlation between CDI and STI, indicating worsened or more severe drought impacts during this period.

Commented [SK28]: Revision based on Reviewer 2: Comm 8

Commented [SK29]: Revision based on Reviewer 2: Comm 9
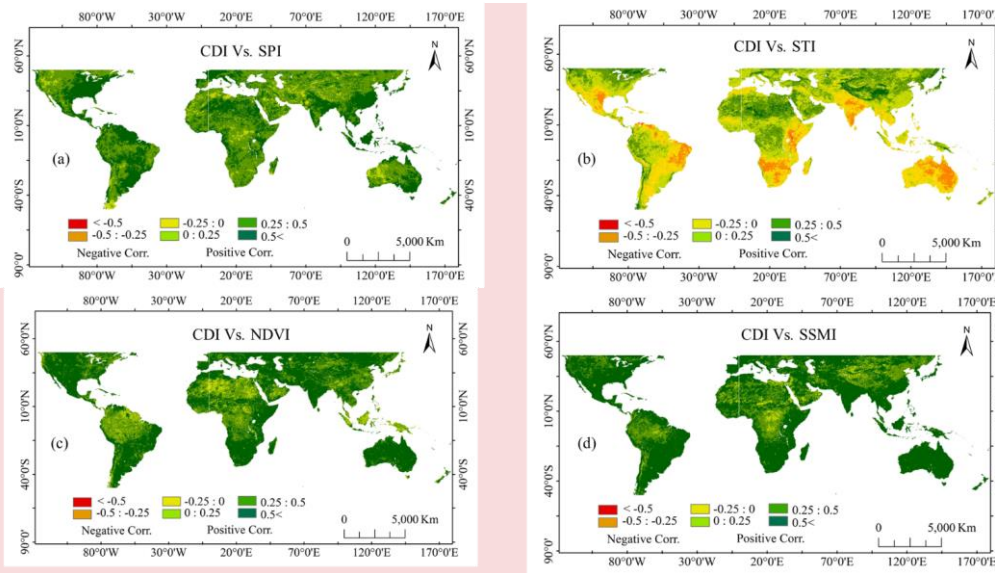
565 **Figure 9.** Spatial correlation between CDI and single input-based traditional indices for a sample month (April): (a) CDI vs. SPI, (b) CDI vs. STI, (c) CDI vs. NDVI, and (d) CDI vs. SSMI. Negative correlations are represented in shades from yellow to red, while positive correlations are shown in shades from light green to dark green.

5. Discussion

One major challenge in drought studies is assessing the aftereffects and propagation of specific drought events on society and
570 their long-term impacts. Some researchers have attempted to shed light on this issue, using proxies to show the socio-economic effects. Noel et al. (2020) compared weekly hazard maps with socio-economic impacts across the USA, and Bachmair et al. (2016) described thresholds for hydrometeorological droughts to understand the socio-economic impacts of droughts in Germany and the U.K. However, these studies were region-specific and insufficient to provide a global perspective. Our study addressed this research gap with the help of GDIS data. The use of GDIS data in this study allowed us to obtain precise
575 subnational information on disaster locations, and instead of relying on proxies, this dataset provided direct on-ground impact information. Consistent with the findings of Kageyama and Sawada (2022), our study also observed that Sub-Saharan Africa and South Asia experienced a higher number of GDIS drought events, highlighting the high vulnerability of these regions to droughts and their socio-economic repercussions.

580 Previous studies, whether regional or global, often relied on single-parameter-based indices for drought monitoring, such as SPI (Ji and Peters, 2003; Liu et al., 2022; Mckee et al., 1993). Each of these has limitations for understanding drought. For instance, SPI is commonly used, but its effectiveness depends heavily on the selected time scale. Shorter time scales, such as SPI-1 and SPI-3, are effective for detecting meteorological and agricultural droughts, respectively, while longer time scales (e.g., SPI-6 or SPI-12) are more suitable for identifying hydrological droughts. However, in regions with distinct wet and dry

585 seasons, SPI can sometimes misrepresent actual drought conditions, for example, a short-term SPI may indicate drought during a naturally dry season, even when annual water availability remains within normal limits. Regarding NDVI, results may vary depending on the type of vegetation, as different plants respond differently to drought stress, which may not always be captured by NDVI. Additionally, particularly in places with abundant rainfall, NDVI may not be able to differentiate between dense vegetation and healthy vegetation. Soil moisture index has limitations in its spatial coverage and the variability of its levels

590 over time, which can respond differently to changing conditions. Hence, the development of CDI in our study and its analysis on a global scale marks a significant departure from previous studies (Ji and Peters, 2003; Liu et al., 2022; Mckee et al., 1993) that focused on single input parameters. By integrating multiple parameters for the analysis, CDI offers a more comprehensive understanding of drought conditions, transcending the limitations inherent in single-parameter approaches. Bayissa et al. (2022), Jiao et al. (2019), and Kulkarni et al. (2020), etc. employed a comprehensive approach, emphasizing the importance

595 of CDI in their regional drought monitoring studies over Sri Lanka, India, and the USA, respectively. However, these studies were limited to regional analyses. Hence, in this study, taking a step ahead, we analyzed droughts using the CDI technique at the subnational level on a global scale.

While some regional studies have used socio-economic data such as crop prices or agricultural losses for drought monitoring (Brown and Funk, 2008; Lobell and Burke, 2010; Wang et al., 2022) we exclude such variables to avoid overlapping with

600 GDIS, which already reflects socio-economic drought events. Our focus is on evaluating how well agro-climatological indices capture these events. Additionally, globally consistent socio-economic datasets are limited, making climate-based indicators more practical for large-scale drought monitoring.

In this study, the computation of CDI-based droughts involved implementing the PCA technique to assign weights to each

605 input parameter. In contrast, previous researchers (Kulkarni et al., 2020b; Thomas et al., 2016) relied on the expert judgment method or copula method (Shah and Mishra, 2020; Tosunoglu and Can, 2016) to assign weights for the input parameters. The expert judgment method is highly subjective, and weight assignments can fluctuate based on individual opinions. Furthermore, the Copula method is more susceptible to outliers, potentially leading to biased weight assessments compared to PCA. Our study addressed these limitations by employing the PCA technique. PCA enhances the assessment of drought severity by

610 objectively identifying influential variables and capturing data patterns, thereby enhancing the accuracy and reliability of our findings.

Commented [SK31]: Revision based on Reviewer 1: Comm 7

Commented [SK32]: Technical Correction 28: Reviewer 3

Commented [SK33]: Revision based on Reviewer 2: Comm 2

The comparative analysis between the CDI and other individual parameter-based indices suggests that CDI offers a strong overall capability for detecting GDIS events, showing robust performance across time windows and a closer association with socio-economic impacts. Inconsistencies between the CDI and other indicators may stem from the different mechanisms these indices use to detect droughts versus the actual ground conditions. One such inconsistency was observed in the Horn of Africa, where the CDI and other indices identified a GDIS drought event, but the SPI did not. This discrepancy could be due to less pronounced precipitation anomalies in the SPI for this region, where baseline rainfall is already low and may not reflect drought conditions accurately. Additionally, it is possible that the observed impact was not solely related to meteorological drought but rather to agricultural or hydrological drought. Factors such as reduced soil moisture, land degradation, or soil types with low water retention capacity captured by SSMI, STI, NDVI, and CDI may have played a more significant role in triggering the event. Another example is from North Argentina (South America), where the SSMI failed to detect a drought that was identified by other indices. This disparity might be due to the presence of the Paraná River, the second-largest river in South America, which provides a significant source of soil moisture. Therefore, the SSMI might not reflect drought conditions. However, it is also possible that the impact was not directly related to soil moisture but instead resulted from meteorological factors such as reduced rainfall or elevated temperatures, which could lead to drought and socio-economic stress, as reflected in GDIS. A further example is from Ballia (Uttar Pradesh, India), where the SPI and SSMI did not detect a GDIS drought, but the NDVI and CDI did. Ballia is near the Ganga River, which supplies ample soil moisture to the surrounding areas. However, the NDVI is particularly effective at identifying droughts in highly vegetated areas due to its sensitivity to precipitation, and soil moisture and its inverse correlation with temperature. Thus, the drought was detected by the NDVI and CDI. The current CDI primarily reflects agro-environmental droughts due to the nature of its input indices. However, since it combines precipitation, temperature, soil moisture, and vegetation data, it may also capture broader drought signals relevant to urban systems, such as water availability and heat stress (Vicente-Serrano et al., 2012; Hao & Singh, 2015; Wang et al., 2020). In future work, we aim to enhance CDI by incorporating sector-specific indicators to better assess socio-economic impacts beyond agriculture.

Through this study, we observed that the relationship between hazard (CDI) and socio-economic impacts (GDIS) is significantly more complex than initially anticipated. The relationship between CDI and GDIS, as well as their vulnerability to drought, varies markedly between developed and less developed regions. Despite some areas in North America and Europe having lower CDI values (less than or equal to -1.5), these regions have not exhibited corresponding GDIS (socio-economic repercussions of droughts) droughts. Conversely, relatively higher CDI values (less than or equal to -1.0 or even -0.5 in some cases) over South Africa or parts of Asia and South America have led to noticeable GDIS events (socio-economic impacts). Meaning that, the threshold values of drought impacts (CDI) differ across regions. These findings align with previous studies (Tanoue et al., 2016; Tschumi and Zscheischler, 2020), which represent the behavior of developed versus developing nations, showing that, although developed nations may experience significant climate anomalies relative to their local climatic norms, they are generally less socio-economically impacted by droughts than developing countries, which tend to be more vulnerable

Commented [SK34]: Revision based on Reviewer 2: Comm 7

Commented [SK35]: Technical Correction 29: Reviewer 3

Commented [SK36]: Technical Correction30: Reviewer 3

Commented [SK37]: Revision based on Reviewer 1: Comm 4

due to limited adaptive capacity. To support this notion, Tanoue et al. (2016) mentioned that vulnerability is associated with the gross domestic product (GDP) of a region, with higher GDP (Europe, North America) indicating less vulnerability and lower GDP (South Africa, South America, South Asia) indicating greater vulnerability.

650

Similarly, Birkmann et al. (2022), Chen et al. (2020), Lavell et al. (2012) claimed that developed regions, with their robust infrastructure, diversified economies, and social safety nets, are better equipped to cope with drought impacts compared to less developed regions with limited resources and institutional capacities. For instance, developed countries may have access to advanced irrigation systems and drought insurance schemes, whereas less developed countries often rely heavily on rainfed

655 agriculture and face greater challenges in mitigating drought impacts. By understanding the association between CDI and GDIS, our study helped to highlight the disparities and complex dynamics of drought hazard and vulnerability between developed and developing nations. These insights could be used to inform area-specific policy implementation and management practices. By integrating multiple indicators, CDI provides a more comprehensive view of drought conditions that is useful for identifying at-risk areas. For example, in regions like East Africa or Central India, where both rainfall deficits

660 and vegetation stress are common during droughts, CDI captures these multiple dimensions more effectively than single-parameter indices. Its regionalized structure ensures better alignment with local climate dynamics, enhancing its potential utility in forecasting and policy targeting. With adaptation to near-real-time inputs, the CDI framework could support early warning systems and guide proactive measures such as crop insurance triggers or water allocation planning. While this study focused on false-negative cases using GDIS as a reference, a systematic assessment of false-positive cases remains challenging.

665 This is due not only to the lack of defined temporal frames for reverse analysis but also to the incomplete coverage of drought impacts in GDIS, especially in developing regions where many drought events may go unreported. These limitations could be addressed in future research using more comprehensive and high-resolution impact datasets.

Although 96% of GDIS events aligned with CDI, there were a few GDIS events that CDI could not capture. This indicates

670 that there was socio-economic stress during these periods, but it was not due to hydro-climatological drought hazards. Other factors must have contributed to this stress. One such event was observed in Burundi (Africa) from June 2001 to December 2001 and in Uganda and Swaziland in southern Africa. Another inconsistent GDIS event was noticed in Peru (South America) in 2010 and Thailand in 2005, when no significant CDI anomalies were observed, yet these periods were noted in the GDIS dataset. These observations demand a more detailed analysis of these events and an understanding of the regional

675 characteristics that might have led to these discrepancies.

The association between the CDI and the GDIS is one of the key takeaway messages of our study, as it directly addresses the gap in understanding actual drought hazards and their socio-economic impacts. However, there are some limitations to this study. One of the primary limitations is the incompleteness of GDIS data. Although GDIS provides valuable information on

680 impacts, the dataset only covers 60% of events registered in EM-DAT at the subnational level. Neither EM-DAT nor GDIS

Commented [SK38]: Revision based on Reviewer 1: Comm 13

Commented [SK39]: Revision based on Reviewer 1: Comm 11

Commented [SK40]: Revision based on Reviewer 1: Comm 10

can cover all disaster details and impacts comprehensively. Additionally, EM-DAT data sometimes lacks exact start and end dates for certain disasters, which might mislead the analysis. Hence, there is still room for improvement in understanding the socio-economic impacts of hazards using accurate datasets or on-ground insights. Emerging approaches such as text mining and natural language processing (NLP) offer promising pathways to address this gap by automatically extracting drought impact information from news articles, institutional reports, and other social media (Fritz et al., 2019; Sathianarayanan et al., 2024), and could serve as alternative or supplementary impact datasets alongside GDIS and EM-DAT. In this study, we developed and compared CDI with the main widely used indices; however, CDI should also be compared with other drought monitoring indices to establish its superiority. One of the other limitations of this research is not considering hydrological variables (groundwater, surface runoff, etc.) in the development of CDI. Due to the limited availability of consistent and high-resolution hydrological data on a global scale, hydrological variables were not included in this study. This may have contributed to certain disparities in detecting GDIS events. While regional high-resolution modeled datasets (e.g., LISFLOOD in Europe) are available, the lack of globally consistent and validated hydrological data remains a constraint. In future work, we will aim to incorporate hydrological variables for computing CDI weights to further improve drought detection and its link to socio-economic events. Further, other alternative methods such as entropy weighting, the analytic hierarchy process, or machine learning-based feature importance (like random forests) could also be explored to compute weights in CDI, as they may better capture indicator relevance by incorporating data variability, expert knowledge, or nonlinear relationships with observed impacts.

6. Conclusion

Droughts rank among the most dangerous natural disasters, influencing a wide array of factors both directly and indirectly, with significant impacts on various socio-economic sectors. Despite numerous techniques and indices for analyzing the physical characteristics of droughts, the methods for understanding their direct socio-economic impacts remain underexplored, particularly at subnational levels. Our study addressed this research gap by investigating the direct propagation of agro-climatological droughts to socio-economic impacts using the GDIS dataset, which provides socio-economic disaster information. Although several indices exist for drought assessment, many rely on single input parameters and fail to consider a comprehensive range of contributing factors, limiting their effectiveness in representing the socio-economic impacts of droughts. To address this limitation, we developed a new Combined Drought Indicator (CDI) that integrates two agricultural (Soil Moisture and NDVI) and two meteorological (Rainfall and Temperature) variables to assess drought conditions. The comparative analysis indicates that the proposed index performs consistently well across different drought scenarios and offers

Commented [SK41]: Revision based on Reviewer 1: Comm 12

Commented [SK42]: Technical Correction 32: Reviewer 3

Commented [SK43]: Revision based on Reviewer 1: Comm 14

Commented [SK44]: Technical Correction 33: Reviewer 3

a more integrated representation of drought patterns, showing a strong association with observed GDIS events and potential

715 links to socio-economic impacts. The takeaway messages from this study can be summarized as follows:

- Globally, the multiparameter approach of the CDI proves to be a highly useful tool for assessing agro-climatological droughts compared to commonly used single-parameter-based traditional indicators such as SPI, SSMI, NDVI, and STI.

720 - CDI-derived drought clusters show strong spatial and temporal association with GDIS-reported drought events, with approximately 95% of GDIS events successfully identified using the CDI. This suggests that the index effectively captures drought conditions that frequently align with documented socio-economic impacts.

- The GDIS dataset provides direct socio-economic hazard event information and can be a valuable validation tool for drought indices.

725 - Regions characterized by the highest frequencies of drought events, as identified by GDIS and multiple indices, including CDI, are predominantly located in Sub-Saharan Africa, South Asia, South America, and Central America, underscoring the heightened vulnerability of these areas to drought occurrences.

This study underscores the applicability of CDI in analyzing droughts with enhanced precision compared to individual indices, effectively capturing their socio-economic repercussions. The direct usability of this technique worldwide could advance

730 drought monitoring systems and inform policy development aimed at addressing both the socio-economic and agro-climatological impacts of droughts.

735

Data availability

All data and codes are available from the corresponding authors upon request.

740

Author contributions

SK and YS designed the study, with SK executing the work. SK prepared the manuscript with contributions from YS, YB, and BW. YS secured the funding.

745 **Competing interests**

The authors declare that they have no conflict of interest.

Commented [SK45]: Revision based on Reviewer 2: Comm 10

Commented [SK46]: Revision based on Reviewer 2: Comm 11

Commented [SK47]: Technical Correction 34: Reviewer 3

Acknowledgments

We gratefully acknowledge the financial support provided by the Japan Aerospace Exploration Agency (grant nos. ER3AMF106), JSPS KAKENHI grant (21H01430 and 24K17352), the Japan Society for the Promotion of Science (grant no. 21H01430), and the Katsu Kimura Research Award for enabling this research.

Financial support

Japan Aerospace Exploration Agency (grant nos. ER3AMF106), JSPS KAKENHI grant (21H01430 and 24K17352), the Japan Society for the Promotion of Science (grant no. 21H01430), and the Katsu Kimura Research Award.

References

CHIRPS: Rainfall Estimates from Rain Gauge and Satellite Observations | Climate Hazards Center - UC Santa Barbara: https://www.chc.ucsb.edu/data/chirps, last access: 20 September 2023.

Drought Impact Reporter (DIR) | Drought.gov: https://www.drought.gov/data-maps-tools/drought-impact-reporter-dir, last access: 26 March 2025.

European Drought Impact Report Inventory (EDII) and European Drought Reference (EDR) database - European Drought Centre: https://europeandroughtcentre.com/news/european-drought-impact-report-inventory-edii-and-european-drought-reference-edr-database/, last access: 26 March 2025.

European Drought Observatory (EDO) — European Environment Agency: https://www.eea.europa.eu/policy-documents/european-drought-observatory-edo, last access: 26 March 2025.

Bachmair, S., Stahl, K., Collins, K., Hannaford, J., Acreman, M., Svoboda, M., Knutson, C., Smith, K. H., Wall, N., Fuchs, B., Crossman, N. D., and Overton, I. C.: Drought indicators revisited: the need for a wider consideration of environment and society, https://doi.org/10.1002/wat2.1154, 1 July 2016.

Bayissa, Y., Srinivasan, R., Joseph, G., Bahuguna, A., Shrestha, A., Ayling, S., Punyawardena, R., and Nandalal, K. D. W.: Developing a Combined Drought Index to Monitor Agricultural Drought in Sri Lanka, Water (Switzerland), 14, https://doi.org/10.3390/w14203317, 2022.

Bayissa, Y. A., Tadesse, T., Svoboda, M., Wardlow, B., Poulsen, C., Swigart, J., and Van Andel, S. J.: Developing a satellite-based combined drought indicator to monitor agricultural drought: a case study for Ethiopia, GIsci Remote Sens, 56, 718–748, https://doi.org/10.1080/15481603.2018.1552508, 2019.

Bhunia, P., Das, P., and Maiti, R.: Meteorological Drought Study Through SPI in Three Drought Prone Districts of West Bengal, India, Earth Systems and Environment, 4, 43–55, https://doi.org/10.1007/s41748-019-00137-6, 2020.

Birkmann, J., Jamshed, A., McMillan, J. M., Feldmeyer, D., Totin, E., Solecki, W., Ibrahim, Z. Z., Roberts, D., Kerr, R. B., Poertner, H. O., Pelling, M., Djalante, R., Garschagen, M., Leal Filho, W., Guha-Sapir, D., and Alegría, A.: Understanding

780 human vulnerability to climate change: A global perspective on index validation for adaptation planning, Science of the Total Environment, 803, https://doi.org/10.1016/j.scitotenv.2021.150065, 2022.

Blain, G. C., da Rocha Sobierajski, G., Weight, E., Martins, L. L., and Xavier, A. C. F.: Improving the interpretation of standardized precipitation index estimates to capture drought characteristics in changing climate conditions, International Journal of Climatology, 42, 5586–5608, https://doi.org/10.1002/joc.7550, 2022.

785 Bolten, J. D., Crow, W. T., Jackson, T. J., Zhan, X., and Reynolds, C. A.: Evaluating the Utility of Remotely Sensed Soil Moisture Retrievals for Operational Agricultural Drought Monitoring, IEEE J Sel Top Appl Earth Obs Remote Sens, 3, 57–66, https://doi.org/10.1109/JSTARS.2009.2037163, 2010.

Brooks, N., Adger, W. N., and Kelly, P. M.: The determinants of vulnerability and adaptive capacity at the national level and the implications for adaptation, Global Environmental Change, 15, 151–163, 790 https://doi.org/10.1016/J.GLOENVCHA.2004.12.006, 2005.

Brown, J. F., Wardlow, B. D., Tadesse, T., Hayes, M. J., and Reed, B. C.: The Vegetation Drought Response Index (VegDRI): A new integrated approach for monitoring drought stress in vegetation, GIsci Remote Sens, 45, 16–46, https://doi.org/10.2747/1548-1603.45.1.16, 2008.

Brown, M. E. and Funk, C. C.: Climate: Food security under climate change, Science (1979), 319, 580–581, 795 https://doi.org/10.1126/SCIENCE.1154102/ASSET/8E0E4B93-2612-4A8C-ADB7-7AB47FA69817/ASSETS/SCIENCE.1154102.FP.PNG, 2008.

Chen, Z., Wang, W., Yu, Z., Xia, J., and Schwartz, F. W.: The collapse points of increasing trend of vegetation rain-use efficiency under droughts, Environmental Research Letters, 15, https://doi.org/10.1088/1748-9326/abb332, 2020.

Christian, J. I., Basara, J. B., Hunt, E. D., Otkin, J. A., Furtado, J. C., Mishra, V., Xiao, X., and Randall, R. M.: Global 800 distribution, trends, and drivers of flash drought occurrence, Nat Commun, 12, https://doi.org/10.1038/s41467-021-26692-z, 2021.

Christian, J. I., Hobbins, M., Hoell, A., Otkin, J. A., Ford, T. W., Cravens, A. E., Powlen, K. A., Wang, H., and Mishra, V.: Flash drought: A state of the science review, https://doi.org/10.1002/wat2.1714, 1 May 2024.

Costanza, J. K., Koch, F. H., and Reeves, M. C.: Future exposure of forest ecosystems to multi-year drought in the United 805 States, Ecosphere, 14, https://doi.org/10.1002/ecs2.4525, 2023.

Ding, Y., He, X., Zhou, Z., Hu, J., Cai, H., Wang, X., Li, L., Xu, J., and Shi, H.: Response of vegetation to drought and yield monitoring based on NDVI and SIF, Catena (Amst), 219, https://doi.org/10.1016/j.catena.2022.106328, 2022.

European Centre for Medium-Range Weather Forecasts: ERA5 Land Monthly Mean Surface Air Temperature, 2023.

Forootan, E., Khaki, M., Schumacher, M., Wulfmeyer, V., Mehrnegar, N., van Dijk, A. I. J. M., Brocca, L., Farzaneh, S., 810 Akinluyi, F., Ramillien, G., Shum, C. K., Awange, J., and Mostafaie, A.: Understanding the global hydrological droughts of 2003–2016 and their relationships with teleconnections, Science of the Total Environment, 650, 2587–2604, https://doi.org/10.1016/j.scitotenv.2018.09.231, 2019.

Fritz, S., See, L., Carlson, T., Haklay, M. (Muki), Oliver, J. L., Fraisl, D., Mondardini, R., Brocklehurst, M., Shanley, L. A., Schade, S., Wehn, U., Abrate, T., Anstee, J., Arnold, S., Billot, M., Campbell, J., Espey, J., Gold, M., Hager, G., He, S., Hepburn, L., Hsu, A., Long, D., Masó, J., McCallum, I., Muniafu, M., Moorthy, I., Obersteiner, M., Parker, A. J., Weissplug, M., and West, S.: Citizen science and the United Nations Sustainable Development Goals, Nature Sustainability 2019 2:10, 2, 922–930, https://doi.org/10.1038/s41893-019-0390-3, 2019.

Grillakis, M. G.: Increase in severe and extreme soil moisture droughts for Europe under climate change, Science of the Total Environment, 660, 1245–1255, https://doi.org/10.1016/j.scitotenv.2019.01.001, 2019.

Guillory, L., Pudmenzky, C., Nguyen-Huy, T., Cobon, D., and Stone, R.: A drought monitor for Australia, Environmental Modelling and Software, 170, https://doi.org/10.1016/j.envsoft.2023.105852, 2023.

Hao, Z., AghaKouchak, A., Nakhjiri, N., and Farahmand, A.: Global integrated drought monitoring and prediction system, Sci Data, 1, 140001, https://doi.org/10.1038/sdata.2014.1, 2014a.

Hao, Z., AghaKouchak, A., Nakhjiri, N., and Farahmand, A.: Global integrated drought monitoring and prediction system, Sci Data, 1, 140001, https://doi.org/10.1038/sdata.2014.1, 2014b.

Hossain Anika Tasnim and MacMurchy, K. and S. J. and S. L.: Creating Water-Secure Futures in Megacities: A Comparative Case Study of `Day Zero' Cities—Bangalore and Chennai, in: The Political Economy of Urban Water Security under Climate Change , edited by: Swatuk Larry and Cash, C., Springer International Publishing, Cham, 105–134, https://doi.org/10.1007/978-3-031-08108-8_5, 2022.

Huang, S., Wang, L., Wang, H., Huang, Q., Leng, G., Fang, W., and Zhang, Y.: Spatio-temporal characteristics of drought structure across China using an integrated drought index, Agric Water Manag, 218, 182–192, https://doi.org/10.1016/j.agwat.2019.03.053, 2019.

Ji, L. and Peters, A. J.: Assessing vegetation response to drought in the northern Great Plains using vegetation and drought indices, Remote Sens Environ, 87, 85–98, https://doi.org/10.1016/S0034-4257(03)00174-3, 2003.

Jiao, W., Tian, C., Chang, Q., Novick, K. A., and Wang, L.: A new multi-sensor integrated index for drought monitoring, Agric For Meteorol, 268, 74–85, https://doi.org/10.1016/j.agrformet.2019.01.008, 2019a.

Jiao, W., Tian, C., Chang, Q., Novick, K. A., and Wang, L.: A new multi-sensor integrated index for drought monitoring, Agric For Meteorol, 268, 74–85, https://doi.org/10.1016/j.agrformet.2019.01.008, 2019b.

Kageyama, Y. and Sawada, Y.: Global assessment of subnational drought impact based on the Geocoded Disasters dataset and land reanalysis, Hydrol Earth Syst Sci, 26, 4707–4720, https://doi.org/10.5194/hess-26-4707-2022, 2022.

Kazemzadeh, M., Noori, Z., Alipour, H., Jamali, S., Akbari, J., Ghorbanian, A., and Duan, Z.: Detecting drought events over Iran during 1983–2017 using satellite and ground-based precipitation observations, Atmos Res, 269, https://doi.org/10.1016/j.atmosres.2022.106052, 2022.

Kogan, F. N.: 1l)lOO, Space Res, 273–1177 pp., 1995.

845 Kulkarni, S. and Gedam, S.: Geospatial approach to categorize and compare the agro-climatological droughts over marathwada region of Maharashtra, India, in: ISPRS Annals of the Photogrammetry, Remote Sensing and Spatial Information Sciences, 279–285, https://doi.org/10.5194/isprs-annals-IV-5-279-2018, 2018.

Kulkarni, S. S., Wardlow, B. D., Bayissa, Y. A., Tadesse, T., Svoboda, M. D., and Gedam, S.: Developing a remote sensing-based combined drought indicator approach for agricultural drought monitoring over Marathwada, India, Remote Sens (Basel),
850 12, https://doi.org/10.3390/rs12132091, 2020a.

Kulkarni, S. S., Wardlow, B. D., Bayissa, Y. A., Tadesse, T., Svoboda, M. D., and Gedam, S. S.: Developing a remote sensing-based combined drought indicator approach for agricultural drought monitoring over Marathwada, India, Remote Sens (Basel), 12, https://doi.org/10.3390/rs12132091, 2020b.

Lavell, A., Oppenheimer, M., Diop, C., Hess, J., Lempert, R., Li, J., Muir-Wood, R., Myeong, S., Moser, S., Takeuchi, K.,
855 Cardona, O. D., Hallegatte, S., Lemos, M., Little, C., Lotsch, A., and Weber, E.: Climate Change: New Dimensions in Disaster Risk, Exposure, Vulnerability, and Resilience, Managing the Risks of Extreme Events and Disasters to Advance Climate Change Adaptation: Special Report of the Intergovernmental Panel on Climate Change, 9781107025066, 25–64, https://doi.org/10.1017/CBO9781139177245.004, 2012.

Liu, Y., Liu, Y., Wang, W., Fan, X., and Cui, W.: Soil moisture droughts in East Africa: Spatiotemporal patterns and climate
860 drivers, J Hydrol Reg Stud, 40, https://doi.org/10.1016/j.ejrh.2022.101013, 2022.

Livada, I. and Assimakopoulos, V. D.: Spatial and temporal analysis of drought in Greece using the Standardized Precipitation Index (SPI), Theor Appl Climatol, 89, 143–153, https://doi.org/10.1007/s00704-005-0227-z, 2007.

Lobell, D. B. and Burke, M. B.: On the use of statistical models to predict crop yield responses to climate change, Agric For Meteorol, 150, 1443–1452, https://doi.org/10.1016/J.AGRFORMET.2010.07.008, 2010.

865 Mckee, T. B., Doesken, N. J., and Kleist, J.: THE RELATIONSHIP OF DROUGHT FREQUENCY AND DURATION TO TIME SCALES, Eighth Conference on Applied Climatology, 17–22 pp., 1993.

Mishra, V.: Long-term (1870–2018) drought reconstruction in context of surface water security in India, J Hydrol (Amst), 580, https://doi.org/10.1016/j.jhydrol.2019.124228, 2020.

Mukherjee, S. and Mishra, A. K.: Global Flash Drought Analysis: Uncertainties From Indicators and Datasets, Earths Future,
870 10, https://doi.org/10.1029/2022EF002660, 2022.

Nam, W. H., Tadesse, T., Wardlow, B. D., Hayes, M. J., Svoboda, M. D., Hong, E. M., Pachepsky, Y. A., and Jang, M. W.: Developing the vegetation drought response index for south korea (Vegdri-skorea) to assess the vegetation condition during drought events, Int J Remote Sens, 39, 1548–1574, https://doi.org/10.1080/01431161.2017.1407047, 2018.

Noel, M., Bathke, D., Fuchs, B., Gutzmer, D., Haigh, T., Hayes, M., Poděbradská, M., Shield, C., Smith, K., and Svoboda,
875 M.: Linking drought impacts to drought severity at the state level, Bull Am Meteorol Soc, 101, https://doi.org/10.1175/BAMS-D-19-0067.1, 2020.

Pak-Uthai, S. and Faysse, N.: The risk of second-best adaptive measures: Farmers facing drought in Thailand, International Journal of Disaster Risk Reduction, 28, 711–719, https://doi.org/10.1016/J.IJDRR.2018.01.032, 2018.

Panwar, V. and Sen, S.: Disaster Damage Records of EM-DAT and DesInventar: A Systematic Comparison, Econ Disaster
Clim Chang, 4, 295–317, https://doi.org/10.1007/s41885-019-00052-0, 2020.

Peel, M. C., Finlayson, B. L., and Mcmahon, T. A.: Hydrology and Earth System Sciences Updated world map of the Köppen-
Geiger climate classification, Hydrol. Earth Syst. Sci, 1633–1644 pp., 2007.

Reyniers, N., Osborn, T. J., Addor, N., and Darch, G.: Projected changes in droughts and extreme droughts in Great Britain
strongly influenced by the choice of drought index, Hydrol Earth Syst Sci, 27, 1151–1171, https://doi.org/10.5194/hess-27-
1151-2023, 2023.

Rosvold, E. and H. Buhaug.: GDIS, a global dataset of geocoded disaster locations, Sci Data, 8,
https://doi.org/10.1038/S41597-021-00846-6, 2021.

Sánchez, N., González-Zamora, Á., Martínez-Fernández, J., Piles, M., and Pablos, M.: Integrated remote sensing approach to
global agricultural drought monitoring, Agric For Meteorol, 259, 141–153, https://doi.org/10.1016/j.agrformet.2018.04.022,
2018.

Sandeep, P., Obi Reddy, G. P., Jegankumar, R., and Arun Kumar, K. C.: Monitoring of agricultural drought in semi-arid
ecosystem of Peninsular India through indices derived from time-series CHIRPS and MODIS datasets, Ecol Indic, 121,
https://doi.org/10.1016/j.ecolind.2020.107033, 2021.

Sathianarayanan, M., Hsu, P. H., and Chang, C. C.: Extracting disaster location identification from social media images using
deep learning, International Journal of Disaster Risk Reduction, 104, 104352, https://doi.org/10.1016/J.IJDRR.2024.104352,
2024.

Sawada, Y.: Quantifying drought propagation from soil moisture to vegetation dynamics using a newly developed
ecohydrological land reanalysis, Remote Sens (Basel), 10, https://doi.org/10.3390/rs10081197, 2018.

Sehgal, V., Sridhar, V., and Tyagi, A.: Stratified drought analysis using a stochastic ensemble of simulated and in-situ soil
moisture observations, J Hydrol (Amst), 545, 226–250, https://doi.org/10.1016/j.jhydrol.2016.12.033, 2017.

Sepulcre-Canto, G., Horion, S., Singleton, A., Carrao, H., and Vogt, J.: Development of a Combined Drought Indicator to
detect agricultural drought in Europe, https://doi.org/10.5194/nhess-12-3519-2012, 2012.

Shah, D. and Mishra, V.: Integrated Drought Index (IDI) for Drought Monitoring and Assessment in India, Water Resour Res,
56, https://doi.org/10.1029/2019WR026284, 2020.

Svoboda, M., Lecomte, D., Hayes, M., Heim, R., Gleason, K., Angel, J., Rippey, B., Tinker, R., Palecki, M., Stooksbury, D.,
Miskus, D., and Stephens, S.: The Drought Monitor, Bull Am Meteorol Soc, 1181–1190, 2002.

Svoboda, M., Hayes, M., and Wood, D.: Standardized precipitation index: user guide., 2012.

Tanoue, M., Hirabayashi, Y., and Ikeuchi, H.: Global-scale river flood vulnerability in the last 50 years, Sci Rep, 6,
https://doi.org/10.1038/srep36021, 2016.

Tao, L., Ryu, D., Western, A., and Boyd, D.: A new drought index for soil moisture monitoring based on MPDI-NDVI
trapezoid space using modis data, Remote Sens (Basel), 13, 1–20, https://doi.org/10.3390/rs13010122, 2021.

Thomas, T., Jaiswal, R. K., Galkate, R., Nayak, P. C., and Ghosh, N. C.: Drought indicators-based integrated assessment of drought vulnerability: a case study of Bundelkhand droughts in central India, Natural Hazards, 81, 1627–1652, https://doi.org/10.1007/s11069-016-2149-8, 2016.

915 Tosunoglu, F. and Can, I.: Application of copulas for regional bivariate frequency analysis of meteorological droughts in Turkey, Natural Hazards, 82, 1457–1477, https://doi.org/10.1007/s11069-016-2253-9, 2016.

Udmale, P., Ichikawa, Y., S. Kiem, A., and N. Panda, S.: Drought Impacts and Adaptation Strategies for Agriculture and Rural Livelihood in the Maharashtra State of India, Open Agric J, 8, 41–47, https://doi.org/10.2174/1874331501408010041, 2014.

Vicente-Serrano, S. M., Beguería, S., and López-Moreno, J. I.: A multiscalar drought index sensitive to global warming: The

920 standardized precipitation evapotranspiration index, J Clim, 23, 1696–1718, https://doi.org/10.1175/2009JCLI2909.1, 2010.

Vicente-Serrano, S. M., Peña-Angulo, D., Beguería, S., Domínguez-Castro, F., Tomás-Burguera, M., Noguera, I., Gimeno-Sotelo, L., and El Kenawy, A.: Global drought trends and future projections, Philosophical Transactions of the Royal Society A: Mathematical, Physical and Engineering Sciences, 380, https://doi.org/10.1098/rsta.2021.0285, 2022.

Wang, H., Liu, H., and Wang, D.: Agricultural Insurance, Climate Change, and Food Security: Evidence from Chinese

925 Farmers, Sustainability (Switzerland), 14, https://doi.org/10.3390/su14159493, 2022.

Wang, T. and Sun, F.: Integrated drought vulnerability and risk assessment for future scenarios: An indicator based analysis, Science of the Total Environment, 900, https://doi.org/10.1016/j.scitotenv.2023.165591, 2023.

Zhang, Q., Li, J., Singh, V. P., and Bai, Y.: SPI-based evaluation of drought events in Xinjiang, China, Natural Hazards, 64, 481–492, https://doi.org/10.1007/s11069-012-0251-0, 2012.

930

935

Appendix A: Stepwise procedure for assessing the consistency of gridded drought indices with GDIS drought events.

Commented [SK48]: Revision based on Reviewer 1: Comm 8

Step	Description
1	For each GDIS event, extract the spatial polygon and event time range (referring to EM-DAT for event details)
2	Extract monthly gridded index values (SPI, STI, SSMI, NDVI, CDI) within a polygon
3	Compute the monthly spatial average of index values within a polygon

4	Check if any month in the event has an average value below a threshold
5	If yes, mark that index as consistent with the GDIS event

Appendix B: PCA-derived monthly weight maps for individual input variables.
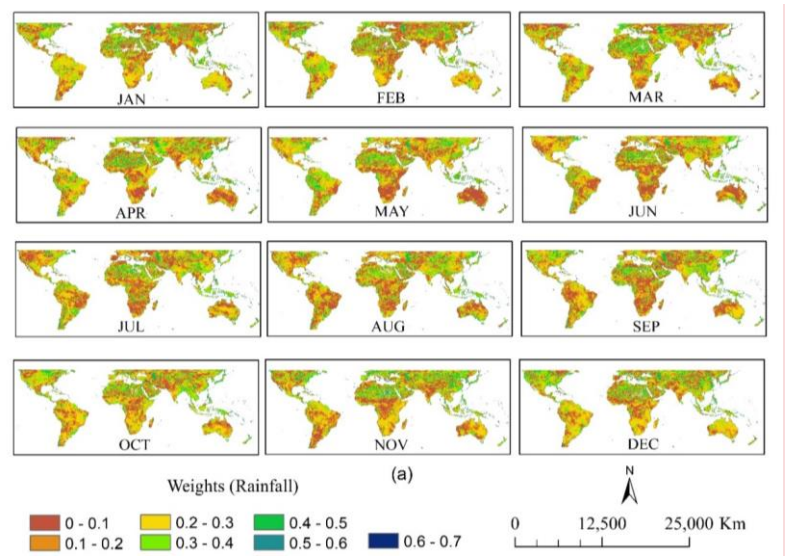
Figure B1. Monthly spatial distribution of PCA-derived weights for rainfall (a), Colour scales indicate the relative contribution of each variable to CDI (brown = low weight, green = moderate weight, blue = high weight).

945
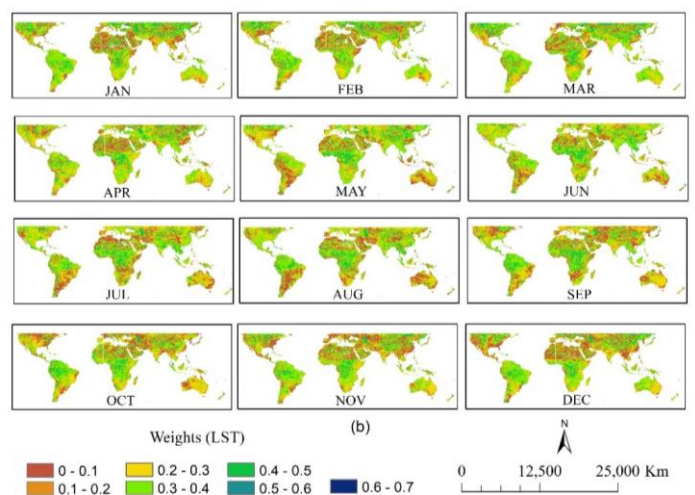
Figure B2. Monthly spatial distribution of PCA-derived weights for temperature (b), Colour scales indicate the relative contribution of each variable to CDI (brown = low weight, green = moderate weight, blue = high weight).
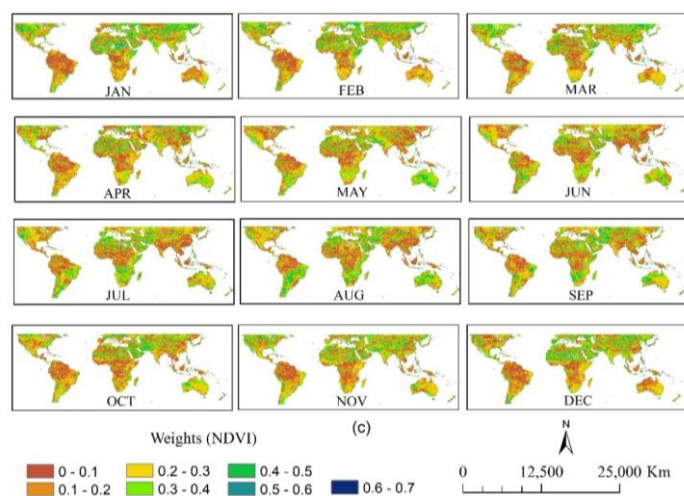
950 **Figure B3.** Monthly spatial distribution of PCA-derived weights for NDVI (c), Colour scales indicate the relative contribution of each variable to CDI (brown = low weight, green = moderate weight, blue = high weight).
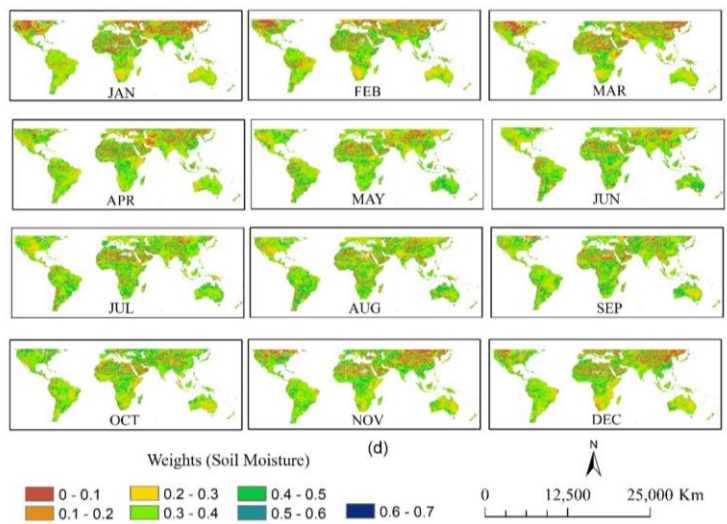
Figure B4. Monthly spatial distribution of PCA-derived weights for soil moisture (d), Colour scales indicate the relative contribution of each variable to CDI (brown = low weight, green = moderate weight, blue = high weight).

Commented [SK49]: Revision based on Reviewer 1: Comm 9
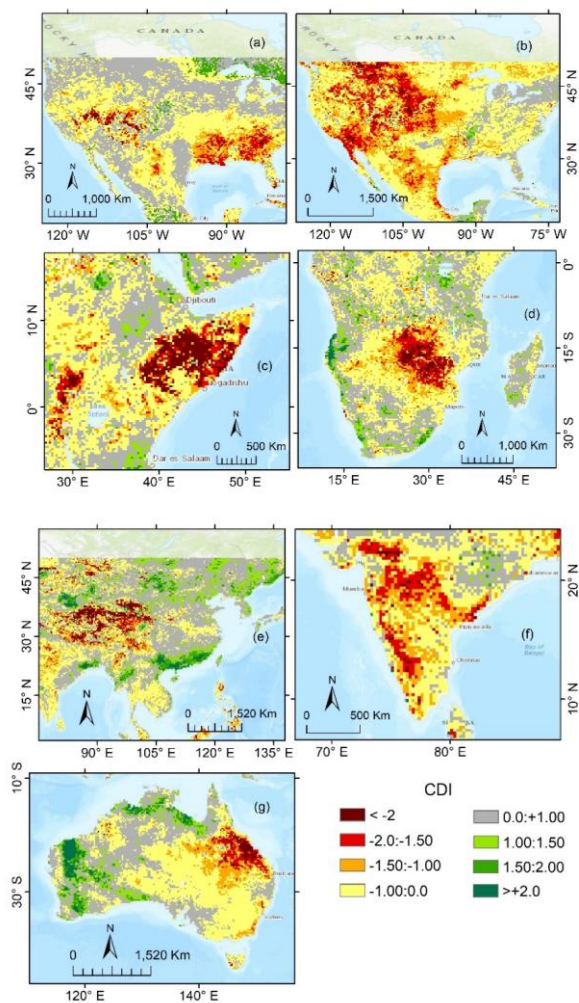
Appendix C: Significant drought events detected by CDI in various global regions include: (a) the USA in August 2007 and
970   (b) July 2012, (c) the Horn of Africa in July 2015, (d) Malawi and Zambia in February 2016, (e) western and northern China
in July 2015, (f) India in July 2015, and (g) Australia in January 2019.
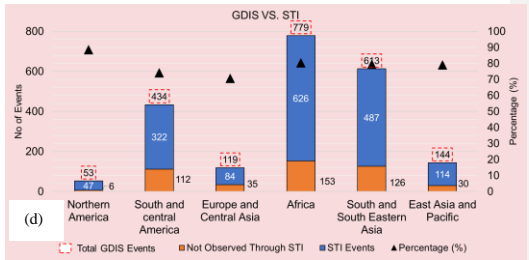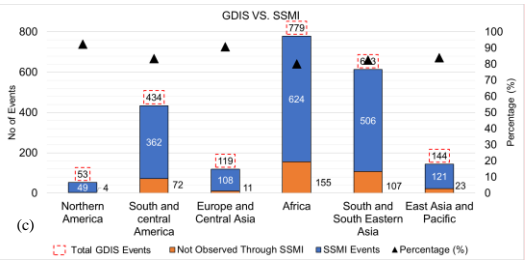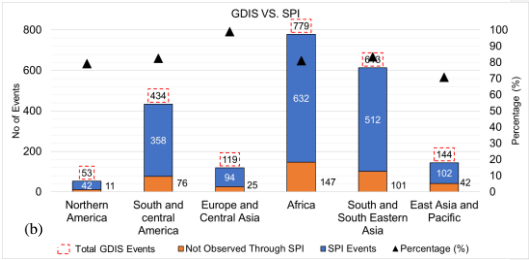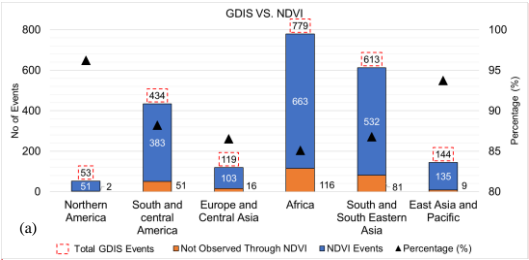
Appendix D: Performance of Traditional Drought Indices in Capturing GDIS Events Across Global Regions: Comparative
Assessment of (a) NDVI, (b) SPI, (c) SSMI, and (d) STI
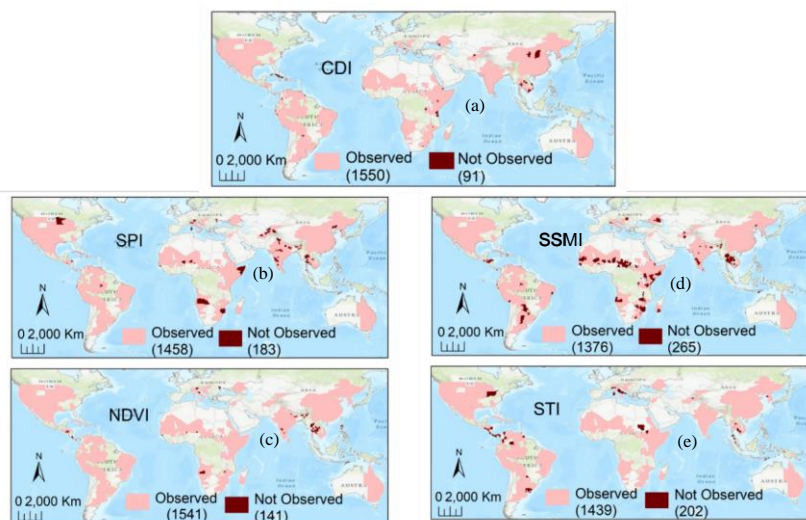
Appendix E: Spatial locations-wise performance of CDI (a), SPI (b), NDVI (c), SSMI (d), and STI (e) in detecting GDIS events, where consistent events detected by each index are shown in pink, while inconsistent GDIS events (not observed) are shown in dark brown. The drought identification criteria were set to events during the actual drought period without considering short droughts (total GDIS events count = 1641).

Appendix F: Performance of traditional drought indices in detecting GDIS events using multiple criteria.

Table F1. Performance of SPI in detecting GDIS events using multiple criteria.

SPI vs GDIS	Total Event	Drought Criteria	Actual Event Period (AEP)		One Month Prior + AEP		Two Month's Prior + AEP		Three Month's Prior + AEP	
			-1	0	-1	0	-1	0	-1	0
Including Short Drought	2142	Observed %	1740	2114	1886	2140	1898	2142	1973	2142
		Not Observed %	402	28	256	2	206	0	160	0
No Short Drought (event >=2 months)	1641	Observed %	1458	1641	1522	1641	1550	1641	1586	1641
		Not Observed %	183	0	119	0	91	0	82	0

Table F2. Performance of SSMI in detecting GDIS events using multiple criteria.

SSMI vs GDIS	Total Event	Drought Criteria	Actual Event Period (AEP)		One Month Prior + AEP		Two Month's Prior + AEP		Three Month's Prior + AEP	
			-1	0	-1	0	-1	0	-1	0
Including Short Drought	2142	Observed %	1770	2106	1912	2130	1936	2140	1988	2142
		Not Observed %	372	36	230	12	206	2	154	0
No Short Drought (event >=2 months)	1641	Observed %	1376	1632	1572	1640	1580	1641	1610	1641
		Not Observed %	265	9	69	1	61	0	31	0

Table F3. Performance of NDVI in detecting GDIS events using multiple criteria.

NDVI vs GDIS	Total Event	Drought Criteria	Actual Event Period (AEP)		One Month Prior + AEP		Two Month's Prior + AEP		Three Month's Prior + AEP	
			-1	0	-1	0	-1	0	-1	0
Including Short Drought	2142	Observed %	1867	2104	1983	2116	2028	2125	2003	2142
		Not Observed %	205	38	159	26	114	17	100	0
No Short Drought (event >=2 months)	1641	Observed %	1541	1622	1561	1626	1574	1627	1576	1641
		Not Observed %	100	19	80	15	67	14	52	0

1010

Table F4. Performance of STI in detecting GDIS events using multiple criteria.

STI vs GDIS	Total Event	Drought Criteria	Actual Event Period (AEP)		One Month Prior + AEP		Two Month's Prior + AEP		Three Month's Prior + AEP	
			-1	0	-1	0	-1	0	-1	0
Including Short Drought	2142	Observed %	1680	2114	1740	2136	1820	2138	1810	2140
		Not Observed %	462	28	292	6	272	4	131	2
No Short Drought (event >=2 months)	1641	Observed %	1439	1619	1479	1628	1510	1654	1556	1603
		Not Observed %	202	22	162	13	131	7	85	0

1015
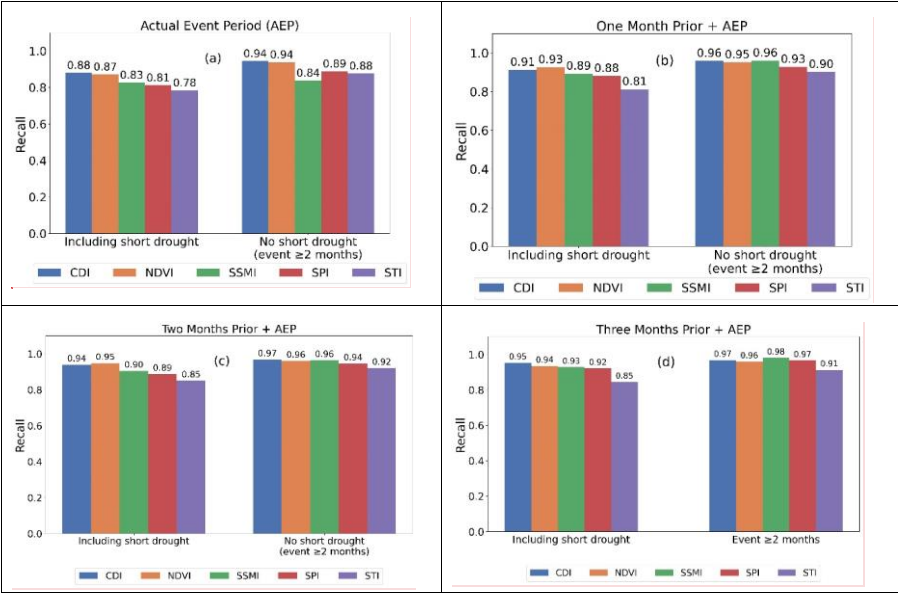
1020 **Appendix G**: Comparative performance recall of five drought indices (CDI, NDVI, SSMI, SPI, and STI) across different time windows and event durations.
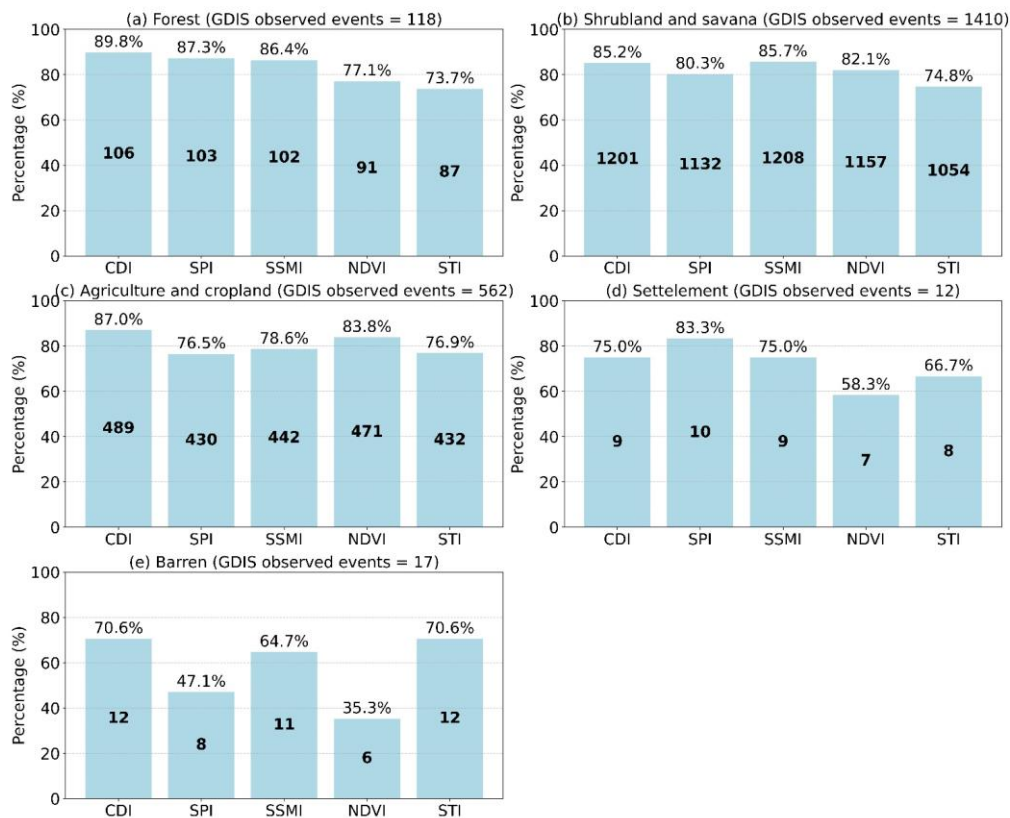
Appendix H: Land cover–wise accuracy of drought indices (CDI, SPI, SSMI, NDVI, STI) in detecting GDIS events across five major land cover classes (Forest, Shrubland and Savanna, Agriculture and Cropland, Settlement, and Barren) based on MODIS land cover data. The bar heights represent the percentage of GDIS events accurately captured, while values inside the bars indicate the absolute number of consistent detections. The total number of GDIS events considered per land cover class is Forest – 118, Shrubland and Savanna – 1410, Agriculture and Cropland – 562, Settlement – 12, Barren – 17.